CrystEngComm

Accepted Manuscript

ROYAL SOCIETY OF CHEMISTRY

www.rsc.org/crystengcomm

Understanding the amino ↔ imino tautomeric preference in (imidazole)imidazolidine-N-aryl(alkyl) systems: a case study of moxonidine drug and insights from Cambridge Structural Database (CSD).

Jagadeesh Babu Nanubolu,*[a] Balasubramanian Sridhar,[a] Krishnan Ravikumar*[a]

[a]Centre for X-ray Crystallography, CSIR-Indian Institute of Chemical Technology, Hyderabad, India, 500607. E-mail: jagadeesh81@gmail.com and sshiya@yahoo.com

Keywords: tautomer, conformer, hydrogen bond, amino, imino, energy, conjugation, double bond, stability, preference.

Abstract

Crystals of moxonidine and its hydrochloride are grown in polar solvents and subjected them to single crystal X-ray diffraction. Base crystallizes in the monoclinic *C*2/*c* space group and hydrochloride salt crystallizes as monohydrate in the orthorhombic *Pbca* space group. Protonation in HCl salt occurs at the imino N-atom of 2-imino-imidazolidine group and results in clear changes in the bond angles and bond distances from the neutral structure. Both structures adopt perpendicular conformations and exhibit a certain degree of similarities in the way the homo and hetero dimer units are connected. Moxonidine can exhibit tautomerism along the imidazolidine-N-aryl fragment, but only imino tautomer is observed in the crystal. Density Functional Theory (DFT) calculations in the gas phase suggest amino tautomer to be highly unstable by 5.74 kcal.mol^{-1} over imino and this perhaps caused it more difficult to observe. 180 crystal structures bearing *(imidazole)imidazolidine-N-aryl(alkyl)* fragment are culled from the Cambridge Structural Database (CSD) to understand if there are any molecular features which can be correlated with the tautomeric occurrence in the crystal. We noticed that conjugation has pronounced effect on the tautomer stability and its occurrence. Structures are divided into four categories based on the location of double bond towards endo or exocyclic N atoms. In category (i), amino tautomer is stabilized with 98.1% success rate, because double bonds participate in conjugation towards endocyclic N atoms. Conversely, in category (ii), conjugation is established towards exocyclic N atoms and stabilizes the imino tautomer with 93.1% success. When conjugation is allowed towards endo and exocyclic N sides (category (iii)) or absent (category (iv)), both amino and imino tautomers are observed. Other important factors such as intramolecular hydrogen bonds and intermolecular hydrogen bonds in the crystal have shown to influence the tautomeric existence and we illustrate these features through

selected examples. Tautomer energy calculations are performed on selected examples from four categories and their relative stabilities are correlated with their observation in the crystals. We also demonstrate how the in-depth structural analysis of CSD helps us to revise two incorrectly determined structures reported earlier. The amino tautomeric form of XIBPOO is corrected to its protonated form with its co-former formamide corrected formate anion in its crystal lattice. Similarly the amino tautomeric form of QABDON is corrected to its imino tautomer.

Graphical Abstract

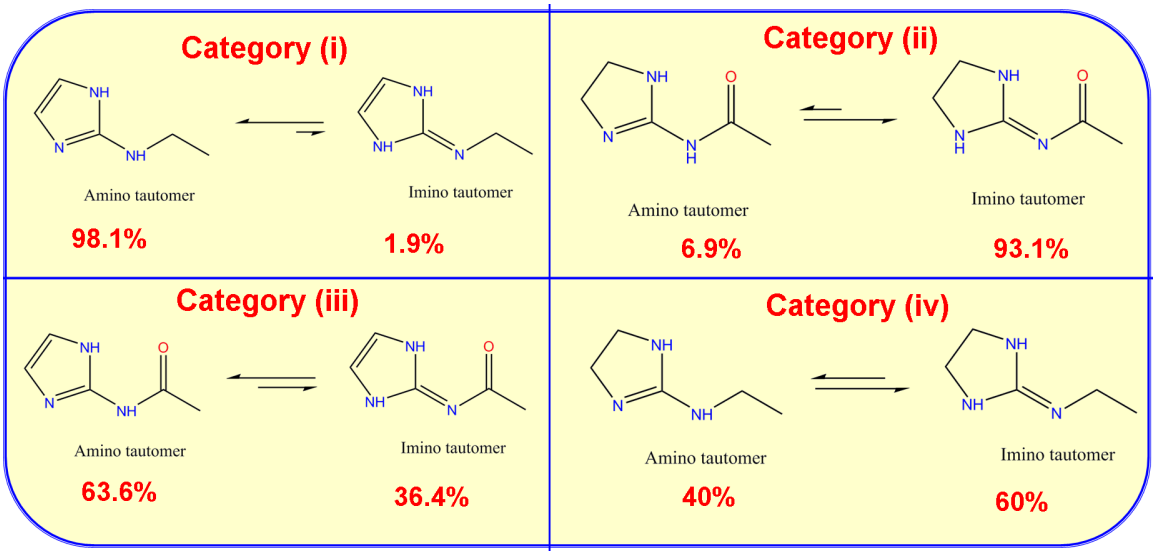

Antihypertensive drug Moxonidine is chosen as a case study to discuss amino ↔ imino tautomerism in imidazolidine-N-aryl systems. Analysis of 180 closely related structures from Cambridge Structural Database (CSD) indicates conjugation is an important factor in deciding which of the two tautomers is stabilized in the crystal structure. Categories (i) and (ii) have high precedence of a single tautomer because conjugation is allowed only on one side, whereas categories (iii) and (iv) are populated with both tautomers because conjugation is either allowed or absent towards both endo and exocyclic N atoms.

Introduction

Tautomerism is the ability of certain organic molecules to exist in isomeric structures which are related by the movement of an atom, usually the hydrogen atom, with simultaneous rearrangement of the double bond.[1] One of the commonly encountered example is keto-enol tautomerism,[1-2] resulting from the migration of a hydrogen atom from carbon to oxygen [O=C-CH_3 ↔ HO-C=CH_2]. The relative population of tautomers depends on temperature, dielectric constant of the medium, and solvents ability to engage in hydrogen bonding.[1] On the other hand, structural isomers which also have the same molecular formula but differ in their atom connectivity do not interconvert in solution.[1b] Classic examples are fumaric and maleic acids. In biology, tautomers of nucleobases play a pivotal role in hydrogen bonding interactions and stabilize the DNA structure.[3] Adenine usually pairs with thymine through amino form and likewise cytosine pairs with guanine through amino tautomer. Mutations in the DNA are thought to arise from tautomeric alterations and unusual base pairing.[3d-f] Many commercial drugs such as sulfamethazine, sulfathiazole, triclabendazole, fenobam, and etc. exist in different tautomeric forms.[4] These exhibit distinct physicochemical profiles and have considerable effect on the drug formulations. Tautomers can also have intellectual property implications as seen with the Ranitidine HCl case study.[4e] Considering the importance of tautomerism in the pharmaceutical industry, identification of the correct tautomer is recognized as one of the important tasks in pharmacophore based virtual screening and drug discovery programs.[5] Recently, tautomer-enriched screening data sets have shown significant advantages in obtaining the perfect fit towards biologically relevant interactions over the non-enhanced sets and suggest a way to increase the number of potential hits.[5a]

In this manuscript, we chose antihypertensive drug moxonidine for studying tautomerism.[6] Moxonidine contains a five membered imidazolidine ring and a six membered pyrimidine ring. Both these rings are connected by a central bridging nitrogen atom. Our interest in this drug arose because of its medicinal importance[6b] and structural implications for amino ↔ imino tautomerism along the cyclic guanidine fragment.[7] The two tautomers are shown in figure 1. In the imino form, double bond is present outside the five membered ring (exocyclic) with both N atoms of the imidazolidine ring containing one proton each, whereas in the amino form, double bond is migrated inside five membered ring (endocyclic) and accordingly proton migrates to bridging N atom. The drug exerts antihypertensive effect by acting on the central nervous system through binding with imidazoline type 1 receptor (I1) in the rostral ventrolateral medulla (RVLM).[6,7] Moxonidine was approved for use in Germany in 1991 and is currently available in Europe and UK, marked by Solvay pharmaceuticals under the brand name Physiotens.[6b-c] Clonidine and α-methyldopa were formerly

prescribed as antihypertensive drugs, but these drugs have sufficient affinity towards α2-adrenergic receptors and cause unwanted side effects such as dry mouth and sedation. Moxonidine showed higher affinity and better selectivity for imidazoline I1 receptor sites than for α2-adrenergic receptors, which resulted in minor side effects compared to clonidine.[7-8]

We use single crystal X-ray diffraction method to study tautomerism in the solid state and gas-phase Density Functional Theory (DFT) calculations to understand the relative energy difference between moxonidine tautomers. Conformational and hydrogen bonding features of moxonidine are discussed in the context of crystal packing and are compared with moxonidine hydrochloride crystal structure (Figure 1). Moxonidine exists only as imino tautomer. Though there are literature reports discussing amino ↔ imino tautomerism in closely related molecules,[9] plausible structural reasons are not clearly understood. To undertake this task, we probed into Cambridge Structural Database (CSD)[10] to obtain significant number of crystal structures, and then to see if there are any molecular features which influence tautomer stability in the solid-state. From the analysis of 180 structures, the role of conjugation, molecular environment, and intra- and inter-molecular hydrogen bonds is clearly evident on the tautomeric stability. Two wrongly determined structures (XIBPOO[11a] and QABDON[11b]) are corrected.

Experimental Section

Crystal growth: Moxonidine and its hydrochloride salt (In-house sources) were recrystallized from methanol using solvent evaporation method. Plate and needle type crystals were obtained after 3-4 days. Best crystals were selected for single crystal X-ray diffraction analysis.

Single crystal X-ray diffraction (SC-XRD):

The intensity data were collected at room temperature using a Bruker Smart Apex CCD diffractometer with graphite monochromated MoKα radiation (λ=0.71073Å) by the ω-scan method. Preliminary lattice parameters and orientation matrices were obtained from four sets of frames. Integration and scaling of the intensity data were accomplished using the program SAINT.[12a] The structures were solved by direct methods using SHELXS97 and refinement was carried out by full-matrix least-squares method using SHELXL97.[12a-b] Anisotropic displacement parameters were calculated for all non-hydrogen atoms. All N-bound H atoms were located in the difference Fourier density map and refined isotropically. The C-bound H atoms in both forms were located in the difference density maps but were positioned geometrically and included as

riding atoms, with C—H = 0.93–0.98 Å , and with U_{iso}(H) = 1.5U_{eq}(C) for methyl H atoms and 1.2U_{eq}(C) for other C-H atoms. The methyl groups were allowed to rotate to optimize the fit of H atoms to the observed electron density. Refinement of XIBPOO structure[11a] is as follows. The CIF and FCF files were downloaded from IUCr page. PLATON[12c] was used to generate RES files from FCF and CIF file. The structure refinement was carried out in Bruker ShelxTL plus.[12a] R*eported crystal data of XIBPOO:* $C_{10}H_{13}ClN_4O$, *M* = 240.69, monoclinic, space group $P2_1/c$ (No. 14), *a* = 8.5840(5), *b* = 13.2740(4), *c* = 9.9080(7) Å, β = 105.789(5)°, *V* = 1086.36(10) Å^3, *Z* = 4, D_c = 1.472 g/cm^3, F_{000} = 504, MoKα radiation, λ = 0.71073 Å, *T* = 150(2)K, $2\theta_{max}$ = 57.0^o, 2655 reflections collected, 2655 unique, Final *GooF* = 0.986, ***R1* = 0.0418, *wR2* = 0.1015**, *R* indices based on 2035 reflections with I >2σ(I) (refinement on F^2), 145 parameters, μ= 0.336 mm^{-1}. *Revised crystal data of XIBPOO structure:* $C_{10}H_{12}ClN_3O_2$, *M* = 241.68, monoclinic, space group $P2_1/c$ (No. 14), *a* = 8.5840(5), *b* = 13.2740(4), *c* = 9.9080(7) Å, β = 105.789(5)°, *V* = 1086.36(10) Å^3, *Z* = 4, D_c = 1.478 g/cm^3, F_{000} = 504, MoKα radiation, λ = 0.71073 Å, *T* = 150(2)K, $2\theta_{max}$ = 57.0^o, 2655 reflections collected, 2655 unique, Final *GooF* = 1.016, ***R1* = 0.0335, *wR2* = 0.0741**, *R* indices based on 2035 reflections with I >2σ(I) (refinement on F^2), 149 parameters, μ = 0.340 mm^{-1}.

Computations: Gaussian09 software[13a] was used for geometry optimization of moxonidine tautomers in the gas phase. All computations were performed using the DFT method with Truhlar's M062x hybrid-meta-GGA functional[13b] at 6-311++G(d,p) basis set level. Representative examples from categories (i) to (iv) are chosen and their imino and amino tautomer energies are estimated using the method described above.

Cambridge Structural Database (CSD)[10] analysis: Two fragments, schematically shown in figure S1 of Electronic Supplementary Information (ESI), are used for querying into the CSD. All bonds in the query fragments including five membered imidazolidine and bridging CN bond are specified as "any" to extract all structures with single, double and resonance structures. Besides, certain filters such as structures with 3D coordinates, no errors, no polymeric, no powder structures, and only organic category are applied to extract good quality crystal structures. The query fragment extracted 827 crystal structures. All ionic structures are excluded leaving 640 hits. All repeated structures and structures where tautomerism is not possible (because hydrogen atoms attached to N atoms are substituted by other groups, N-R) are manually removed. In some structures like IMAFEN, LENREB, QIBBIM, REJVAE01, TARZUH and XEQXAT, the tautomeric fragment sits exactly on two fused five membered rings, which can be analyzed as both amino and imino tautomer. Addition of these compounds does not allow the correct statistical representation; hence, we prefer to exclude them. Applying these tight filters has resulted in a total of 180 structures. 107 structures are represented as amino tautomer (59.4%) and 73 are imino tautomer structures

(40.6%). Please see Table S1 of ESI for refcodes in these two categories. The segregation of tautomers is achieved by applying bond distance criteria as C=N for imino and C-N-H for amino tautomer. The tautomer probability in each of these categories is analyzed. In category (i), out of 53 structures, 52 structures exist as amino tautomer and 1 structure takes imino tautomer and the probability of occurrence is 98.1% for amino and 1.9% for imino tautomer. In category (ii), out of 47 structures, 42 structures are represented as imino tautomer and 5 structures as amino tautomer (ABPHAK10, AHOXOL, HACJUR, UNUMEW and XIBPOO), of which the last two structures are found to be wrong. Excluding these two structures, the estimated probability of occurrence is 93.1% (42 out of 45) for imino tautomer and 6.9% (3 of 45) for amino tautomer. In category (iii), a total of 75 structures are analyzed, of which, SEDZUW and SEFBAG are excluded because of inaccurate inter-atomic bond distances. The probability of occurrence for amino tautomer is 63.6% (46 out of 73) and for imino tautomer is 36.4% (27 of 73). The QABDON of category (iii) is wrongly assigned as amino tautomer which should otherwise be imino tautomer. In category (iv), out of 5 structures, the amino tautomer is seen in 2 structures with 40% probability of occurrence and 3 structures are imino tautomers with 60% probability of occurrence.

Results and Discussion

Crystal structures description: We adopted solvent screening method for moxonidine drug using several polar and non-polar organic solvents, such as methanol, ethanol, n-propanol, i-propanol, n-butanol, water, dimethyl formamide, dimethyl sulfoxide, acetonitrile, chloroform, ethyl acetate and various combinations of solvents to grow suitable crystals for single crystal diffraction analysis. Some co-crystallization experiments were also performed with aromatic and inorganic acids. These experiments resulted in the suitable crystals of base (I) from methanol and its hydrochloride salt (II) from methanol-water. The outcome of various other crystallization experiments was the repeated observation of moxonidine base as confirmed by unit cell check on the single crystal X-ray diffractometer. No polymorphs or pseudo-polymorphs were identified. Although the crystal structure of free base (I) has been mentioned in a patent,[14] its co-ordinates are not available in the Cambridge Structural Database (CSD). A determination of the structure was necessary to establish a direct comparison with the hydrochloride salt. Influence of molecular conformation and hydrogen bonding patterns are established in two crystal structures.

Moxonidine crystallizes in the monoclinic centrosymmetric space group *C*2/*c* with a single molecule in the asymmetric unit (Figure 2a & Table 1). The imidazolidine ring exists in a half-chair conformation. Out of two possible tautomers, only the imino tautomer is present in the solid state (Figure 1). The

torsion angles between imidazolidine and pyrimidine rings indicate a perpendicular orientation (Table 2), with a dihedral angle of 88.91˚ between the planes of pyrimidine and imidazoline rings. Two types of N-H…N dimers are observed. The first dimer is a homo-dimer formed between two imidazolidine rings related by inversion via N4-H4N…N3 interaction (Figure 3a, Table 3). The graph-set notation[15] for this motif is $R_2^2(8)$. The second dimer is a hetero-dimer observed between imidazolidine NH and pyrimidine N by strong N5-H5N…N2 interactions (Figure 3b, Table 3). The H-bond motif can be defined as $R_2^2(14)$ motif by graph-set notation. The two pyrimidine rings in this hetero-dimer show π…π interactions with a centroid…centroid distance of 3.811(2)Å and a weak C6-H6B…N1 bonding between para-methyl hydrogen and pyrimidine nitrogen (Table 3). The homo and hetero dimers periodically repeat to form an infinite 1D ribbon, linking the two fold and inversion related molecules respectively along the plane parallel to [1 0 -1], as shown in figure 4a. The adjacent polymeric ribbon units are connected by C5-H5B…O3 dimers ($R_2^2(8)$ ring motif) and form a two dimension layer along the *ac* plane, which further links to similar layers above and below by weak C8-H8B…N5 interactions.

Moxonidine hydrochloride (II) crystallizes in the orthorhombic centrosymmetric space group *Pbca* (Table 1). The asymmetric unit contains moxonidine in its protonated form, hydrochloride anion, and a water molecule (Figure 2b). Protonation occurs at the imino N-atom of 2-imino-imidazolidine group and results in clear changes in the bond distances and valence angles around the imidazolidine and bridging N atom (Table 2). Some trends are apparent: (i) lengthening of exocyclic N3-C7 double bond by 0.034Å and shortening of endocyclic single bonds C7-N5 and C7-N4 by 0.041 and 0.068Å respectively, indicating the loss of double bond character in the former and gain of double bond character in the latter two bonds. (ii) The valence angle around the bridging nitrogen atom (C4-N3-C7) has widened by 8˚ whereas two angles along the imidazolidine ring-bridging N atom (N3-C7-N4 and N3-C7-N5) have narrowed by 2-3˚. (iii) The pyramidal N4 and N5 atoms (sp^3 hybridized) and planar N3 atom (sp^2 hybridized) in (I) adopt an equivalent planar geometry in (II). It can be inferred that all three nitrogen atoms gain partial sp^2 hybridization as result of the positive charge delocalization across the bonds in the cyclic guanidine fragment (Figure 1). (iv) The half chair conformation of imidazolidine ring in (I) becomes planar in (II) because the carbon atoms are attached to sp^2 hybridized N atoms in the protonated form, whereas they are attached to sp^3 hybridized N atoms in the neutral imino tautomer.

Similar to moxonidine base, the protonated moxonidine exhibits perpendicular orientation of imidazolidine and pyrimidine rings (dihedral angle of 89.13˚ between two rings) and the two types of dimers noticed in (I) are also noticed in the salt (II) but with adjustments made to accommodate water and Cl anion. Two

N-H…N interactions of imidazolidine-imidazolidine homo-dimer in (I) are interrupted by chloride ions and form four N-H…Cl interactions (Figures 5a and 3a). Similarly, two N-H…N interactions in imidazolidine-pyrimidine hetero-dimer of (I) are interrupted by water and chloride ion and form a combination of N-H…O, O-H…N, N-H…Cl and O-H…Cl interactions in the hydrochloride salt (Figure 5b and 3b). It can be noticed that the smaller chloride anion and water molecules act as spacers and their donor/acceptor capabilities are adequately utilized to provide somewhat similar dimers, even though moxonidine changes from neutral to protonated states. These two sets of dimers extend as a polymeric 1D ribbon units, which are in turn connected by N-H…O and O-H…Cl interactions to form a two dimensional sheet/layer (Figure 4b). Weak C-H…O interactions assist in the close packing of 2D layers.

Thus the crystal structures of moxonidine and its hydrochloride salt have displayed certain similarities although they differ at their global crystal packing and lead to different space group selection (Table 1). Firstly, it adopts almost similar perpendicular conformation in both neutral and protonated form. Secondly, they form similar sets of imidazolidine homo and hetero N-H…N dimers with adjustments made to incorporate water and hydrochloride anion in between the dimers. Third, a C-H…O dimer in (I) is replaced by O-H…Cl interactions in (II) to connect adjacent one-dimensional polymeric ribbons to two-dimensional layers/sheets. It is interesting to note that such structural similarities are however not observed with a closely related molecular structure, clonidine and its hydrochloride salt which adopt different molecular conformations and hydrogen bonding patterns.[16] Therefore, preference for a perpendicular conformation of moxonidine both in its neutral and protonated form appears to be directly influenced by the formation of similar supramolecular assemblies, as shown in figures 3 and 5. The non-coplanarity of the imidazolidine and aromatic rings is shown to be a prerequisite for drug interactions at the adrenergic receptors for biological activity,[17] and we show herein that moxonidine indeed adopts such a non-coplanar conformation both in its neutral and protonated form.

Tautomer and conformer energies: Geometry optimization of both amino and imino tautomers of moxonidine are performed with Density Functional Theory (DFT) method using Truhlar's M062x hybrid-meta-GGA functional at 6-311++G(d,p) basis set level.[13] In the stable conformation of imino tautomer **I1** (Figure 6), the imidazolidine and pyrimidine rings adopt a non-planar orientation at a dihedral angle of 53.54˚ between the two rings (Table 2). The imidazolidine N-H points towards ortho-methoxy group to form an intramolecular N-H…O hydrogen bond in **I1**. As there is a second ortho substituent on the pyrimidine ring, the molecule can adopt another imino conformation **I2**, in which imidazolidine N-H points towards chlorine atom to

form intramolecular N-H…Cl contact. Computations indicate that **I2** conformation is 0.21 kcal.mol^{-1} higher than **I1.** The imidazolidine and pyrimidine rings are oriented at a dihedral angle of 66.89 kcal.mol^{-1} in **I2**. Neither of these intramolecular hydrogen bonded conformations is observed in the crystal, instead, **I3** conformation with imidazolidine N-H oriented perpendicularly to pyrimidine ring with a dihedral angle of 88.91˚ and devoid of intramolecular hydrogen bonds with ortho substituents is seen. Energy wise, conformation **I3** is 0.94 kcal mol^{-1} higher than **I1** conformation. Such a conformation is preferred in the crystal perhaps to provide stronger intermolecular hydrogen bonds and better close packing of molecules. The bond distances and bond angles are comparable between the experimental and optimized conformations. Similar to imino tautomer of moxonidine, three conformations of amino tautomer are considered for computations, **A1** with endocyclic N-H pointing towards methoxy group, **A2** with endocyclic N-H pointing towards chlorine, and **A3** with endocyclic N-H perpendicular to two ortho substituents. Variations in the orientations of endocyclic N-H and exocyclic N-H are considered. These two N-H can be oriented *anti* (**A1** and **A2**) or *syn* to each other (**A1S** and **A2S**) as shown in figure 6. All amino tautomer conformations have non-planar orientations of the two rings (Table 2) and energy wise they are metastable over imino conformations. Compared to the stable imino **I1**, amino **A1** conformation is higher by 5.74 kcal mol^{-1}, **A2** is higher by 6.07 kcal.mol^{-1}, and **A3**, **A1S, A2S** are even higher by 7-8 kcal.mol^{-1} range. The enhanced stability of imino tautomer is attributed to the delocalization of exocyclic N lone pair and C=N *p*-orbital into the phenyl ring π-system[18] and from also intramolecular hydrogen bond formation. Usually high energy tautomers/conformations are not observed unless there are strong intermolecular forces to compensate for their energy penalty in the crystal structures. Finally, moxonidinium cation was subjected to geometry optimization and was found to be having perpendicular orientation of imidazolidinium and pyrimidine ring, similar to the observed conformation in the crystal structure of (II). An overlay of conformations of (I) and (II) and their optimized conformations in the gas-phase are shown in the figure 7.

CSD analysis: In contrast to the case study of moxonidine presented above, certain molecules in the literature such as urea-imidazole, amidobenzimidazole, oxoimidazolidyl show strong preference for amino tautomers in their crystals.[19] And few others, such as tetrazole-saccharinate, 3,5-dihydroimidazol-4-one, benzimidazolylthioureas exist as both amino and imino tautomers.[20] To understand the plausible structural reasons causing this tautomeric behavior, we probed into Cambridge Structural Database (CSD). Our idea is to obtain statistically significant number of structures containing "*(imidazole)imidazolidine-N-aryl(alkyl)*" fragment from the database and to understand if there are any molecular features which can be linked to the tautomeric preference. A total of 180 crystal structures are analyzed, of which 107 structures are represented as

amino tautomers and 73 structures as imino tautomers (Table S1 of ESI). Please refer to experimental section for detailed querying into CSD. We note that the conjugation seems have pronounced effect on the tautomer stability. A required condition for conjugation is to have minimum of two double bonds separated by a single bond and planarity of atoms for *p*-orbital delocalization.[1] There is already one double bond in the tautomeric fragment or cyclic guanidine fragment (Figure 1) and additional double bond such as C=C, C=O, C=S is required to establish conjugation with it. Four categories of structures are noted (Figure 8) depending on the side bearing the additional double bond for conjugation: *(i) 53 structures containing double bond exclusively towards endocyclic N atoms (ii) 47 structures containing double bond exclusively towards exocyclic N atom (iii) 75 structures containing double bonds towards endo as well as exocyclic N atoms and (iv) 5 structures without double bonds towards both endo and exo sides.*

In category (i) structures with the additional double bond towards endocyclic N atoms, conjugation occurs only in the amino tautomer whereas the double bonds are isolated in the imino tautomer (Figure 8). So as to favor conjugation, the amino tautomer is expected to be more stable and statistical trends in the CSD concur with this observation with 98.1% success rate for amino and only 1.9% for imino tautomer (Figure 9). The stability of amino tautomer is supported by computational calculations on HEDVAP structure which is 5.01 kcal.mol^{-1} lower in energy than the imino tautomer (Figure 10) and is also observed in the crystal. Figure S2 of ESI displays various conjugated fragments stabilizing the amino tautomer, of which, majority of them show aromatic conjugated rings imidazole and benzimidazole (ASOSUX, XUQTOT) and others are linear conjugated systems over two or more double bonds (MACPIM, PIBPEX). In 6 structures, though the double bonds are isolated (NEFRUM, VEHDUH), the N atom in between facilitates conjugation through lone pair involvement[1] and are therefore included here. Interestingly, these 6 structures crystallize as amino tautomer and suggest the role of conjugation on the tautomer stability. XUDPES structure is the only exception which crystallized as imino tautomer in this category (i), perhaps to facilitate infinite chain of bifurcated N-H…O interactions and N-H…N dimers in the crystal (Figure S3 of ESI).

In category (ii) structures with the additional double bond towards exocyclic N atom, conjugation is established only in the imino tautomer, whereas, two double bonds are isolated in the amino tautomer (Figure 8). This situation is quite opposite to category (i), and as a result, the imino tautomer is likely to be more stable. CSD statistical trends reflect the high probability of occurrence for imino tautomer with 93.1% success rate in the category (ii) and only 6.9% for amino tautomer (Figure 9). The higher stability of imino tautomer is further supported by computational calculations on BABBUB, a representative structure from category (ii), which is 10.09 kcal.mol^{-1} lower in energy than the amino

tautomer (Figure 10) and is also observed in the crystal. Figure S4 of ESI displays category (ii) structures containing conjugated fragments over two double bonds or more (IQAFEL, KABFID) and structures stabilized by conjugation + intramolecular N-H…N/O hydrogen bonds with adjacent nitro, carbonyl, pyrimidine and imidazole (PIBGOY, MOKKAZ). Figure S5 of ESI displays 9 structures having close resemblances to moxonidine that they all contain imidazolidine-N-phenyl backbone (MUFBUK, GOLNIE). Interestingly all of them crystallized as imino tautomer except XIBPOO which was reported as amino tautomer[11a] but we corrected this to its protonated form (structure correction part is discussed later). The enhanced stability of imino tautomer in all these cases can be attributed to the conjugation of exocyclic N-lone pair and C=N *p*-orbitals into the phenyl ring π-system[18] and intramolecular N-H…F/Cl hydrogen bond formation with the ortho substituents.[22] Computations also support the stability of imino over amino tautomer by 3.1 kcal.mol^{-1} in 2-phenylamino-2-imidazoline[22a] and by 7.40 kcal.mol^{-1} in clonidine structure (GOLNIE).[22a] There are three exceptions which crystallized as amino tautomer in this category (ii), AHOXOL, HACJUR and ABPHAK10. The plausible reasons are attributed to the ability of these molecules to form intramolecular N-H…O bonds in them (Figure S6 of ESI).

In category (iii) structures with the additional double bonds located towards both endocyclic and exocyclic N atoms, conjugation is established both in the amino and imino tautomers and suggest the possibility of two tautomers. The estimated statistical probabilities reflect this expected trend with 63.6% for amino and 36.4% for imino tautomers in this category (iii). Computations of CIVRUV, a representative structure from category (iii), indicate a 0.37 kcal.mol^{-1} energy difference between two tautomers (Figure 10). Such small energy differences may be easily compensated by crystal forces for optimal crystal packing. It is noted that the side that allows stronger conjugation appears to direct the tautomer in the category (iii). In particular, aromatic conjugation strongly influences and allows amino tautomers to be observed in 39 structures (Figure S7 of ESI). Computing tautomer energies of PIDJOD indicate that amino tautomer with aromatic conjugation is relatively more stable by 4.02 kcal.mol^{-1} over imino tautomer (Figure 12). Interestingly, 15 structures prefer imino tautomer at the cost of aromatic conjugation (Figure S8 of ESI). GEMMAN examples illustrate this point which prefer imino over amino tautomer in the crystals even though it loses aromatic conjugation and is less stable by 2.91 kcal.mol^{-1} over amino (Figure 11). Intermolecular forces play a significant role in the stabilization of such metastable conformers. In systems of non-aromatic conjugated systems, amino tautomer is preferred when the number of conjugated double bonds are relatively higher towards endocyclic N atoms (DEMDAB, XUDNOA), similarly, imino tautomer is preferred when double bonds are higher towards exocyclic N-atom (BAFMUS, LUVPOH) and almost equal populations of both tautomers are

seen when double bonds are equal in number towards both endo and exocyclic N atoms (BOCYOH, MECVAT). Selected structures from this category are shown in Figure S7, S8 of ESI.

In category (iv) structures without the double bond towards both endo and exocyclic N atoms, the influence of conjugation on the tautomer stability is ruled out completely (Figure 8) and thereby allow both tautomers to be observed in this category (iv) with probability of occurrence of 63.6% for amino tautomer and 36.4% for imino tautomer (Figures 9, S9 of ESI). Computations of REJVEI, a representative structure from category (iv), indicate an energy difference of 0.57 kcal.mol^{-1} between two tautomers (Figure 10) and such small energy differences can be easily overcome by crystal forces and the tautomer that promotes the better close packing of molecules in the crystal will be preferred.

To conclude in brief, the tautomeric occurrence in each of the four categories is shown to be dependent on conjugation, aromaticity, chemical environment of the molecule and their ability to form intramolecular hydrogen bonds. It is important to note that the crystal forces, especially intermolecular hydrogen bonding, could play a significant role in stabilizing the tautomers. For example, the amino tautomer of GEMMAN01 is more stable than the imino tautomer by 2.91 kcal.mol^{-1}, however, this is not observed, instead, the metastable imino tautomer is stabilized by intermolecular N-H…O and N-H…N hydrogen bonds in its crystal structures (Figure S10 of ESI). Recently, Lill and Broo[22] have reported that, molecule VI (6-amino-2-phenylsulfonylimino-1,2-dihydropyridine, as a monomer shows strong preference to exist as sulfonamide tautomer by 11 kcal.mol^{-1}, while remarkably the equilibrium shifts towards sulfonimide tautomer in the crystal due to the formation of strong hydrogen bonds for the imide tautomer and environmental effects.[22] As a third example, we invoke HACJOL and HACJUR pair[23] for understanding the role of intermolecular forces on the tautomer occurrence. These two structures differ by iodine ↔ hydroxyl replacement on a remote location (Figure 12). However, this single substitution alters the intermolecular contacts in the crystal and the tautomer choice. The iodine group in HACJUR involves in I…O contacts using the amino tautomer whereas the hydroxyl group in HACJOL forms bifurcated N-H…O and O-H…O contacts using the imino tautomer (Figure S11 of ESI).

Structure corrections: We now present discussion pertaining to wrong tautomeric assignments in two reported structures and how our CSD analysis helps us to arrive at these structure revisits. **XIBPOO:** This CSD refcode relates to crystal structure of N-(4-Chlorophenyl)-N-(4,5-dihydro-1Himidazol-2-yl)amine formamide solvate, reported by S. O. Yildirim et al. in *Acta Crystallogr. Sect E, 2007, 63, o2130*.[11a] This structure is closely related to moxonidine and also eight other structures in category **(ii)** of figure S5 of ESI. Surprisingly, XIBPOO was

reported as amino tautomer when all others have crystallized as imino tautomer. This deviation prompted us to investigate the XIBPOO structure more in detail. To understand the energy difference between the tautomers of XIBPOO, we first performed two separate tautomer energy calculations. The amino tautomer is higher than imino tautomer by 4.15 kcal.mol^{-1}, similar to the relative energy trends observed in moxonidine system. An in-depth crystal packing analysis of XIBPOO does not suggest any stabilizing features to compensate for the high energy penalty of reported amino tautomer. On the contrary, there are H…H repulsive contacts (1.99Å & 2.24 Å) between imidazolidine C-H and N-H of formamide which could actually destabilize the structure (Figure 13a). To probe further, bond distances and angles of XIBPOO are analyzed and compared with optimized tautomers of XIBPOO. Bond distances match neither amino nor imino tautomers (Table 4), and are found to be intermediate and more close to protonated structure of moxonidine hydrochloride (II) in table 2. An optimization of the XIBPOO protonated form was therefore carried out and geometrical bond parameters are compared which further suggests the reported XIBPOO to be in its protonated form.

For the molecule to be protonated, the molecule must have an acidic co-former in the crystal. The co-former in XIBPOO is formamide whose acid dissociation constant is small (pK_a value is 16.67)[24] and may not undergo deprotonation. One possibility is that the assigned co-former may be wrong. This we say because, the observed C-N (1.244Å) and C-O (1.260Å) bond distances of formamide in XIBPOO deviate significantly from those of corresponding bond distances in a reported formamide solvate of isonicotinamide [GAVHER, C-N(1.317Å) and C-O(1.233Å)].[10] The near equality of the bond distances suggests a deprotonated carboxylic acid group, $HCOO^-$, rather than the formamide. Sigma Aldrich catalogue product information sheet of formamide indicates that once the bottle of formamide is opened and exposed to oxygen, this product begins to oxidize to formic acid (product catalogue F9037).[25] Considering this, it could be reasoned that oxidized byproduct formic acid might have crystallized with the XIBPOO and formed a salt. The pK_a of formic acid[24] is 4.2 which suggest the feasibility of deprotonation to formate anion (Figure 13b).

As a final confirmation, we have analyzed the difference Fourier map of the crystal structure. Fortunately, the structure factor file (.fcf) was available and F_o-F_c maps could be generated easily using WingX software.[12d] The difference Fourier map of the slant plane defined by imidazolidine ring atoms is shown in figure 14a. The positive electron density near N2 atom suggests for a missing proton. Figure 14b shows the difference Fourier map of the slant plane defined by formamide atoms. The positive electron density around N4 atom and negative electron density in places where protons were incorrectly placed are indicated. PLATON[12c] was used to generate the res file for crystal structure

refinement. The structure was revised by incorporating the protonation at the imidazolidine ring and replacing the formamide N4 atom to formate anion O2. The crystal structure refined better by lowering its R factor (*R1* reduces from 0.0418 to 0.0335 and *wR2* reduces from 0.1015 to 0.0741 in the revised structure). Experimental section provides the comparison of reported and refined parameters. Difference Fourier maps of the revised structure are generated (Figures 14c and 14d) which clearly indicate that all atoms are now correctly assigned. The H…H repulsive contacts between imidazolidine and formamide NH_2 are replaced as stabilizing C-H…O interactions with formate anion in the revised structure (Figure 13c).

QABDON: This CSD refcode relates to crystal structure of 2-(2,6-dichlorophenylamino)-3,6,6,8-tetramethyl-3H,6H-imidazo[4,5-h]isoquinoline-7,9-dione, reported by R. J. Snow et.al in *J. Med. Chem. 2002, 45, 3394*.[11b] The structure is observed in category (iii) where conjugation can be established towards both endo and exocyclic N atoms sides. The structure was reported as amino tautomer which should be imino tautomer in principle, as shown in figure 15a. We say this because the bridging CN bond distance is 1.296Å, a value typical for C=N bond instead of assigned C-N bond. Further confirmation came from computational optimization of the amino and imino tautomers of QABDON and comparison of geometrical parameters with those of experimental values (Table 5). Stability wise too, the amino tautomer is less stable than the imino tautomer by 9.78 kcal mol^{-1} (Figure 15a). Since there is no structure factor file for this compound, the reported tautomeric form in the CIF file was corrected using CSD mercury software.[26] A crystal packing of the uncorrected and corrected crystal structures are shown in figures 15b and 15c. The imino tautomer allows an intramolecular N-H…O bond with the adjacent isoquinoline-dione group and also an intermolecular N-H…O bond with carbonyl group, shown in figure 15b. Further, the H…H repulsive contact is replaced by stabilizing C-H….N interaction in the revised structure, figure 15c. QABDON is an interesting example to illustrate how the molecule loses aromatic conjugation of amino tautomer in favor of an imino tautomer to facilitate better intra- and intermolecular hydrogen bonds in the crystal. To conclude in brief, we show that reported amino tautomer of XIBPOO is actually a protonated form and reported amino tautomer of QABDON is corrected to imino form. Two recent papers by S. Bekö et al[27] and A. J. Cruz-Cabeza et al[28] which also deal with corrections to reported tautomers are relevant to this study.

Conclusions

Antihypertensive drug moxonidine is chosen as a case study to discuss amino ↔ imino tautomerism in imidazolidine-N-aryl systems. Single crystal X-ray diffraction study of (I) confirms that moxonidine drug exist exclusively as imino tautomer in the solid state. Diverse crystallization experiments performed in search of amino tautomer has always ended up in the imino tautomer. No polymorphs or pseudo-polymorphs could be obtained, but a novel moxonidine hydrochloride monohydrate structure (II) is obtained. A structural comparison of the base with moxonidine salt structure is established. Protonation occurs at the imino N-atom of 2-imino-imidazolidine group and results in clear changes in the bond distances and valence angles around the imidazolidine and bridging N atom. Both structures contain a perpendicular orientation of imidazolidine and pyrimidine rings and exhibit certain similarities in the way homo and hetero dimers are observed in the crystals with suitable adjustments made to accommodate water and Cl anion in the hydrochloride salt (II). Two N-H…N interactions of imidazolidine-pyrimidine dimer in (I) are replaced by four N-H…O, O-H…N, N-H…Cl and O-H…Cl interactions in (II) and two N-H…N interactions of imidazolidine homo-dimer are replaced by four N-H…Cl interactions in (II). Density Functional Theory (DFT) calculations are performed to understand the energy difference between moxonidine tautomers. Both tautomers adopt a non-planar conformation of imidazolidine and pyrimidine rings. The amino tautomer is 5.74 kcal.mol^{-1} higher in energy than the imino tautomer. Observation of such high energy tautomers/conformers with compensation for energy penalty is rare in the solid state.

In contrast to moxonidine which appears as imino tautomer, certain molecules exist only as amino tautomers, and certain others exist as both amino and imino tautomers. Plausible structural reasons for this tautomeric behavior are not clear. To undertake this task, we probed into Cambridge Structural Database (CSD) and 180 structures with *(imidazole)imidazolidine-N-alkyl(aryl)* fragments are analyzed. Amino tautomer is observed predominantly in structures which have double bond towards endocyclic N atoms (category (i)) and imino tautomer is observed predominantly in structures which have double bond towards exocyclic N atoms (category (ii)). The double bond containing side participates in conjugation with the cyclic guanidine fragment and stabilizes the respective tautomers. In structures with double bond on both sides (category (iii)), the stronger conjugation side, in particular aromatic conjugation decides the tautomeric propensity. And when conjugation effects are completely removed (category (iv)), both tautomers are equally populated. The role of molecular environment, choice of intra- and inter-molecular hydrogen bonds in crystals, and importantly conjugation effects are shown to have influence on the tautomeric stability and occurrence in the crystals. We also present corrections to

two wrongly assigned structures in the literature (XIBPOO and QABDON). We believe that consideration of conjugation as an important criterion for determining the predominant tautomeric form could facilitate a better virtual screening of drugs via better optimized fit at the receptor sites.

Acknowledgements

We acknowledge the CSIR, New Delhi, for financial support as a part of XII five-year plan program under the titles AARF (CSC0406) and ORIGIN (CSC0108). We take this opportunity to thank Dr. Tejender S. Thakur from Molecular and Structural Biology Division, CSIR-Central Drug Research Institute for his kind help on computational part and Dr. Yarasi Soujanya from Centre for Molecular Modeling of IICT, for helpful discussions. The director Dr. M. Lakshmi Kantam is thanked for her kind encouragement.

References

1) (a) M. B. Smith and J. March. In Advanced organic chemistry. Wiley, New York, 2001; (b) P. Y. Bruice, In Essential organic chemistry, Pearson Education, 2006; (c) G. Clayden, W. Warren, N. Greeves and P. Wothers, In Organic Chemistry, OUP Oxford publishers, 2001.
2) (a) S. Kandambeth, D. B. Shinde, M. K. Panda, B. Lukose, T. Heine and R. Banerjee, *Angew. Chem. Int. Ed.* 2013, **125**, 13290; (b) P. Sanphui, N. R. Goud, U. B. R. Khandavilli, S. Bhanoth and A. Nangia, *Chem. Commun.* 2011, **47**, 5013.
3) (a) G. M. Blackburn, In Nucleic Acids in Chemistry and Biology, Royal Society of Chemistry, 2006; (b) W. Saenger, In Principles of Nucleic Acid Structure, Springer-Verlag, New York, 1988. (c) R. R. Sinden, In DNA Structure and Function, Academic Press, San Diego, 1994; (d) M. D. Topal, J. R. Fresco, Nature, 1976, **263**, 285. (e) C. Colominas, F. J. Luque and M. Orozco, *J. Am. Chem. Soc.* 1996, **118**, 6811; (f) M. Rueda, F. J. Luque, J. M. López and M. Orozco, *J. Phys. Chem. A*. 2001, **105**, 6575.
4) (a) P. P. Bag, R. R. Kothur and C. M. Reddy, *CrystEngComm*, 2014, **16**, 4706; (b) J. Lu, A. J. Cruz-Cabeza, S. Rohani and M. C. Jennings, *Acta. Crystallogr., Sect. C: Cryst. Struct. Commun.*, 2011, **C67**, o306; (c) S. Tothadi, B. R. Bhogala, A. R. Gorantla, T. S. Thakur, R. K. R. Jetti and G. R. Desiraju, *Chem. –Asian. J.* 2012, **7**, 330. (d) S. P. Thomas, K. Nagarajan and T. N. Guru Row, *Chem. Commun.* 2012, **48**, 10559; (e) M. Mirmehrabi, S. Rohani, K. S. K. Murthy and B. Radatus, *J.Cryst. Growth,* **2004**, *260*, 517.
5) (a) F. Oellien, J. Cramer, C. Beyer, W. Ihlenfeldt and P. M. Selzer, *J. Chem. Inf. Model.* 2006, **46**, 2342; (b) A. R. Katritzky, C. D. Hall, B. El-Dien, M. El-Gendy and B. Draghici, *J. Comput. Aided Mol. Des.* 2010, **24**, 475.
6) (a) S. T. W. Morris and J. L. Reid, *J. Human Hypertension*, 1997, **11**, 629; (b) C. Fenton, G. M. Keating and K. A. Lyseng-Williamson, *Drugs*, 2006, **66**, 477; (c) J. Waters, J. Ashford, B. Jäger, S. Wonnacott and C. N. Verboom, *J. Clin. Basic Cardiol.* 1999, **2**, 219.
7) M. Remko, O. A. Walsh, W. G. Richards, *J. Phys. Chem. A*, 2001, **105**, 6926.
8) A. G. Head, *Ann. N. Y. Acad. Sci.* 1998, **881**, 279.

9) (a) L. Varga, T. Nagy, I. Kövesdi, J. Benet-Buchholz, G. Dormán, L. Ürge and F. Darvas, *Tetrahedron*, 2003, **59**, 655; (b) G. Morel, E. Marchand, A. Foucaud, *J. Org. Chem.* 1990, **55**, 1721.
10) Cambridge Structural Database, ver. 5.32. ConQuest 1.15, November 2013 release, Feb 2014 update, CCDC, www.ccdc.cam.ac.uk
11) (a) S. Ö. Yildirim, M. Akkurt, S. Servi, M. Sekerci, F. W. Heinemann, *Acta. Cryst. Sec. C: Struct. Rep. Online*, 2007, **E63**, o2130; (b) R. J. Snow, M. G. Cardozo, T. M. Morwick, C. A. Busacca, Y. Dong, R. J. Eckner, S. Jacober, S. Jakes, S. Kapadia, S. Lukas, M. Panzenbeck, G. W. Peet, J. D. Peterson, A. S. Prokopowicz III, R. Sellati, R. M. Tolbert, M. A. Tschantz, N. Moss, *J. Med. Chem.* 2002, **45**, 3394.
12) (a) Bruker, SAINT and SMART, Bruker AXS Inc., Madison, Wisconsin, USA, 2001; (b) G. M. Sheldrick, *Acta Crystallogr. Sect. A: Found. Crystallogr.* 2008, **64**, 112; (c) A. L. Spek, *J. Appl. Cryst.* 2003, **36**, 7; (d) L. J. Farrugia, *J. Appl. Cryst.* 2012, **45**, 849.
13) (a) M. J. Frisch, G. W. Trucks, H. B. Schlegel, G. E. Scuseria, M. A. Robb, J. R. Cheeseman, G. Scalmani, V. Barone, B. Mennucci, G. A. Petersson, H. Nakatsuji, M. Caricato, X. Li, H. P. Hratchian, A. F. Izmaylov, J. Bloino, G. Zheng, J. L. Sonnenberg, M. Hada, M. Ehara, K. Toyota, R. Fukuda, J. Hasegawa, M. Ishida, T. Nakajima, Y. Honda, O. Kitao, H. Nakai, T. Vreven, J. A. Montgomery Jr., J. E. Peralta, F. Ogliaro, M. Bearpark, J. J. Heyd, E. Brothers, K. N. Kudin, V. N. Staroverov, R. Kobayashi, J. Normand, K. Raghavachari, A. Rendell, J. C. Burant, S. S. Iyengar, J. Tomasi, M. Cossi, N. Rega, J. M. Millam, M. Klene, J. E. Knox, J. B. Cross, V. Bakken, C. Adamo, J. Jaramillo, R. Gomperts, R. E. Stratmann, O. Yazyev, A. J. Austin, R. Cammi, C. Pomelli, J. W. Ochterski, R. L. Martin, K. Morokuma, V. G. Zakrzewski, G. A. Voth, P. Salvador, J. J. Dannenberg, S. Dapprich, A. D. Daniels, O. Farkas, J. B. Foresman, J. V. Ortiz, J. Cioslowski and D. J. Fox, Gaussian 09, Revision C.01, Gaussian, Inc., Wallingford CT, 2009; (b) Y. Zhao and D. G. Truhlar, *Theor. Chem. Acc.*, 2008, **120**, 215.
14) I. Adin, O. Arad, C. Iustain, J. Kaspi and A. Weisman, Chemagis Ltd, 2008, WO/2008/020425 http://patentscope.wipo.int/search/en/WO2008020425
15) (a) M. C. Etter, J. C. MacDonald and J. Bernstein, *Acta Crystallogr., Sect. B: Struct. Crystallogr. Cryst. Chem.*, 1990, **46**, 256; (b) J. Bernstein, R. R. Davis, L. Shimoni and N.-L. Chang, *Angew. Chem., Int. Ed. Engl.*, 1995, **34**, 1555.
16) (a) G. Byre, A. Mostad, C. Romming, *Acta Chim. Scandinavica*, 1976, **B30**, 843; (b) V. Cody and G. T. DeTitta, *J. Cryst. Mol. Struct.* 1979, **9**, 33; (c) D. Schollmeyer and M. Henk, *Private Communication*, 2002, CSD Refcode MUFBUK.
17) K. Nikolic, S. Filipic and D. Agbaba, *Bioorg. Med. Chem.* 2008, **16**, 7134.
18) (a) L. M. Jackman and T. Jen, *J. Am. Chem. Soc.*, 1975, **97**, 2811; (b) A. P. de Jong, *J. Med. Chem.*, 1980, **23**, 889.
19) (a) A. M. McGhee, J. P. Plante, C. A. Kilner and A. J. Wilson, *Supramol. Chem.* 2011, **23**, 470; (b) J. Karolak-Wojciechowska, A. Mrozek, W. Kwiatkowski, W. Ksiazek, K. Kieć-Kononowicz and J. Handzlik, *J. Mol. Struct.* 1998, **447**, 89.
20) (a) A. Ismael, J. A. Paixão, R. Fausto and M. L. S. Cristiano, *J. Mol. Struct.* 2012, **1023**, 128; (b) J. Karolak-Wojciechowska, E. Szymańska, A. Mrozek, K. Kieć-Kononowicz, *J. Mol. Struct.* 2009, **930**, 126; A. Śmiechowska, W. Przychodzeń, J. Chojnacki, P. Bruździak, J. Namieśnik, A. Bartoszek, *Struct. Chem.* 2010, **21**, 955.

21) (a) M. Remko, P. Th. Van Duijnen, M. Swart, *Struct. Chem.* 2003, **14**, 271; (b) M. Remko, O. A. Walsh, W. G. Richards, Phys. *Chem. Chem. Phys.* 2001, **3**, 901.
22) S. O. N. Lill and A. Broo, *Cryst. Growth. Des.* 2014, **14**, 3704.
23) M. Dennis, L. M. Hall, P. J. Murphy, A. J. Thornhill, R. Nash, A. L. Winters, M. B. Hursthouse, M. E. Light and P. Horton, *Tett. Let.* 2003, **44**, 3075.
24) Marvin, version 5.10.1, ChemAxon, Budapest, 2009, http://www.chemaxon.com.
25) https://www.sigmaaldrich.com/content/dam/sigma-aldrich/docs/Sigma/Product_Information_Sheet/f9037pis.pdf
26) C. F. Macrae, I. J. Bruno, J. A. Chisholm, P. R. Edgington, P. McCabe, E. Pidcock, L. Rodriguez-Monge, R. Taylor, J. van de Streek and P. A. Wood, *J. Appl. Cryst.* 2008, **41**, 466.
27) S. L. Bekö, S. D. Thoms, M. U. Schmidt, and M. Bolte, *Acta. Crystallogr. Sect C: Cryst. Struct. Commun*. 2012, **C68**, o28.
28) A. J. Cruz-Cabeza, C. R. Groom, *CrystEngComm*, 2011, **13**, 93.

Table 1. Crystal data of moxonidine (I) and its hydrochloride salt (II).

Compound reference	Moxonidine (I)	Moxonidinium hydrochloride monohydrate (II)
Chemical formula	$C_9H_{12}ClN_5O$	$C_9H_{13}ClN_5O^+.Cl^-.H_2O$
Formula Mass	241.69	296.16
Crystal system	Monoclinic	Orthorhombic
a/Å	21.293(2)	8.5413(10)
b/Å	7.8312(9)	13.2793(15)
c/Å	13.9098(16)	24.376(3)
α/°	90	90
β/°	109.820(2)	90
γ/°	90	90
Unit cell volume/Å^3	2182.0(4)	2764.8(5)
Temperature/K	294(2)	294(2)
Space group	*C2/c*	*Pbca*
No. of formula units per unit cell, *Z*	8	8
Radiation type	MoKα	MoKα
Absorption coefficient, *μ*/mm^{-1}	0.337	0.472
No. of reflections measured	11106	27121
No. of independent reflections	2203	2795
R_{int}	0.0246	0.0291
Final R_1 values ($I > 2\sigma(I)$)	0.0640	0.0535
Final $wR(F^2)$ values ($I > 2\sigma(I)$)	0.1480	0.1293
Final R_1 values (all data)	0.0656	0.0614
Final $wR(F^2)$ values (all data)	0.1490	0.1346
θ range /˚	2 to 26.3	1.8 to 26.3
Goodness of fit on F^2	1.271	1.166
Largest diff. peak and hole/e Å^3	0.45 and -0.22	0.32 and -0.13
CCDC number	1015876	1015877

Table 2. Selected bond distances (Å), bond angles (˚), torsion angles (˚) and dihedral angles (˚) in the computed amino, imino and protonated forms of moxonidine and their comparison with conformations observed in crystal structures (I) and (II).

	Imino **I1**	Imino **I2**	Imino **I3**	Imino **(I)crystal**	Amino **A1**	Amino **A2**	Amino **A3**	Salt **(II)crystal**	Salt **(II)optimized**
Bond distances along the imidazolidine-N-pyrimidine fragment									
d[C4-N3]	1.382	1.385	1.390	1.406	1.402	1.402	1.402	1.406	1.418
d[N3-C7]	1.281	1.279	1.278	1.284	1.392	1.390	1.375	1.318	1.332
d[C7-N5]	1.383	1.383	1.384	1.354	1.392	1.394	1.399	1.313	1.328
d[C7-N4]	1.380	1.377	1.378	1.362	1.274	1.274	1.275	1.304	1.339
Bond angles along the imidazolidine-N-pyrimidine fragment									
∠[C4-N3-C7]	121.96	119.27	117.78	115.43	123.14	122.62	123.16	123.39	123.34
∠[N3-C7-N5]	130.23	129.49	128.81	128.37	122.17	120.06	118.64	125.23	124.85
∠[N3-C7-N4]	121.83	122.89	123.50	123.77	119.78	122.38	123.85	123.00	124.25
∠[N5-C7-N4]	107.88	107.59	107.69	107.86	118.03	117.53	117.44	111.77	110.90
Torsion angles in the imidazolidine(imidazoline) ring									
τ[C7-N4-C8-C9]	-29.53	28.75	28.10	25.89	-13.87	23.59	24.00	-12.35	-18.43
τ [C7-N5-C9-C8]	-27.14	28.83	28.91	25.32	-20.71	15.69	16.38	-10.97	-20.68
τ [N4-C8-C9-N5]	32.84	-33.25	-32.96	-29.32	21.34	-24.20	-24.87	13.30	22.23
τ [N4-C7-N5-C9]	9.63	-11.92	-12.37	-10.16	14.51	0.11	-0.25	3.64	10.09
τ [C8-N4-C7-N5]	13.66	-11.79	-11.08	-10.95	0.00	-16.58	-16.64	6.14	6.13
Torsion angles and dihedral angles connecting the imidazolidine(imidazoline) and pyrimidine ring									
τ [C1-C4-N3-C7]	56.99	115.89	90.24	87.19	74.55	104.04	85.14	98.37	110.98
τ [C4-N3-C7-N5]	4.62	-6.59	0.91	0.90	-27.66	17.88	0.90	-5.49	3.52
φ[imidazolidine-pyrimidine]	53.54	66.89	88.39	88.91	51.06	61.42	88.32	89.13	69.89

Table 3. Hydrogen bonding and π… π interactions in (I) and (II).

S.No	D-H…A	D-H / Å	H…A / Å	D…A / Å	∠D-H…A
Moxonidine, (I)					
1	N4-H4N…N3^{i}	0.84	2.20	3.038(3)	172(3)
2	N5-H5N…N2^{ii}	0.78	2.29	3.036(3)	162(3)
3	C5-H5B…O3^{iii}	0.96	2.59	3.353(4)	136
4	C6-H6B…N1^{ii}	0.96	2.77	3.563(5)	141
5	C8-H8B…N5^{iv}	0.97	2.68	3.634(5)	167
7	Cg(2)…Cg(2)^{v}	-	-	3.811(2)	-
^{i}1/2-x,3/2-y, -z; ^{ii}1-x, y, 1/2-z; ^{iii}1/2-x, 1/2-y, -z; ^{iv}1/2-x, 1/2+y,1/2-z; ^{v}3/2+x,1/2-y,1/2+z; Cg(2) = centroid of pyrimidine ring atoms.					
Moxonidine hydrochloride monohydrate, (II)					
1	O1W-H1W…N2^{i}	0.79^{i}	2.13	2.911(4)	169(4)
2	O1W-H2W…Cl2^{ii}	0.74^{ii}	2.38	3.119(3)	173(4)
3	N3-H3N…Cl2	0.84	2.18	3.015(3)	175(2)
4	N4-H4N…Cl2^{iii}	0.84^{iii}	2.51	3.149(3)	133(2)
5	N5-H5N…O1W	0.84	1.91	2.723(4)	164(2)
6	C8-H8B…O1^{iv}	0.97	2.68	3.541(3)	148
7	C9-H12B…Cl2^{v}	0.97	2.76	3.543(3)	137
8	Cg(1)…Cg(1)^{iv}	-	-	3.848(2)	-
^{i} -1/2+x,y,1/2-z; ^{ii} -1+x,y,z; ^{iii} 2-x, 1-y, 1-z; ^{iv} 1-x, 1-y, 1-z; ^{v} 3/2-x, 1/2+y, z; Cg(1) = centroid of imidazolidine ring atoms.					

Table 4. Selected bond distances (Å), bond angles (°) in XIBPOO.

S.No	Reported XIBPOO	Amino Optimized	Imino Optimized	Protonated Optimized
d[N1-C7]	1.341	1.376	1.272	1.327
d[C7-N2]	1.329	1.277	1.382	1.333
d[C7-N3]	1.332	1.398	1.388	1.339
∠[C6-N1-C7]	125.24	128.87	119.61	121.98
∠[N1-C7-N3]	126.56	120.37	129.92	125.22
∠[N1-C7-N2]	121.04	122.37	122.98	124.06
∠[N2-C7-N3]	112.40	117.26	107.10	110.73
∠[C7-N2-C8]	111.08	105.89	109.93	110.02
∠[C7-N3-C9]	109.70	104.26	109.48	110.39
φ[imidazolidine-pyrimidine]	43.33	42.83	57.11	87.84

Table 5. Selected bond distances (Å), bond angles (°) in QABDON.

S.No	Reported QABDON	Amino Optimized	Imino Optimized
d[N4-C8]	1.381	1.406	1.388
d[C5-N4]	1.296	1.394	1.280
d[C5-N2]	1.378	1.302	1.384
d[C5-N3]	1.373	1.370	1.382
∠[C8-N4-C5]	120.91	117.61	119.09
∠[N5-C5-N3]	128.99	125.67	130.28
∠[N5-C5-N2]	122.42	119.61	123.74
∠[N2-C5-N3]	108.56	114.69	105.97
φ[imidazole-pyrimidine]	74.09	70.02	68.59

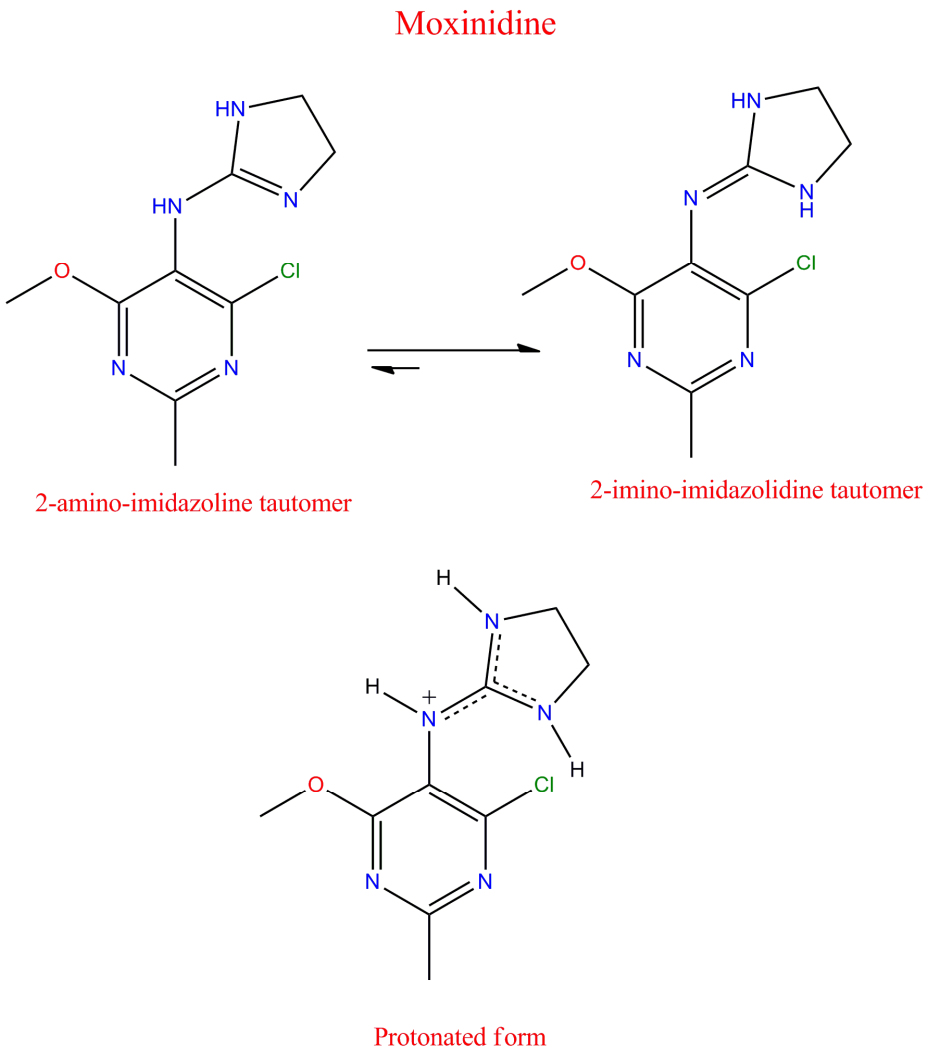

Figure 1. Molecular structures of moxonidine, its tautomers and protonated form. Dotted lines are indicative of charge delocalization in the protonated form.

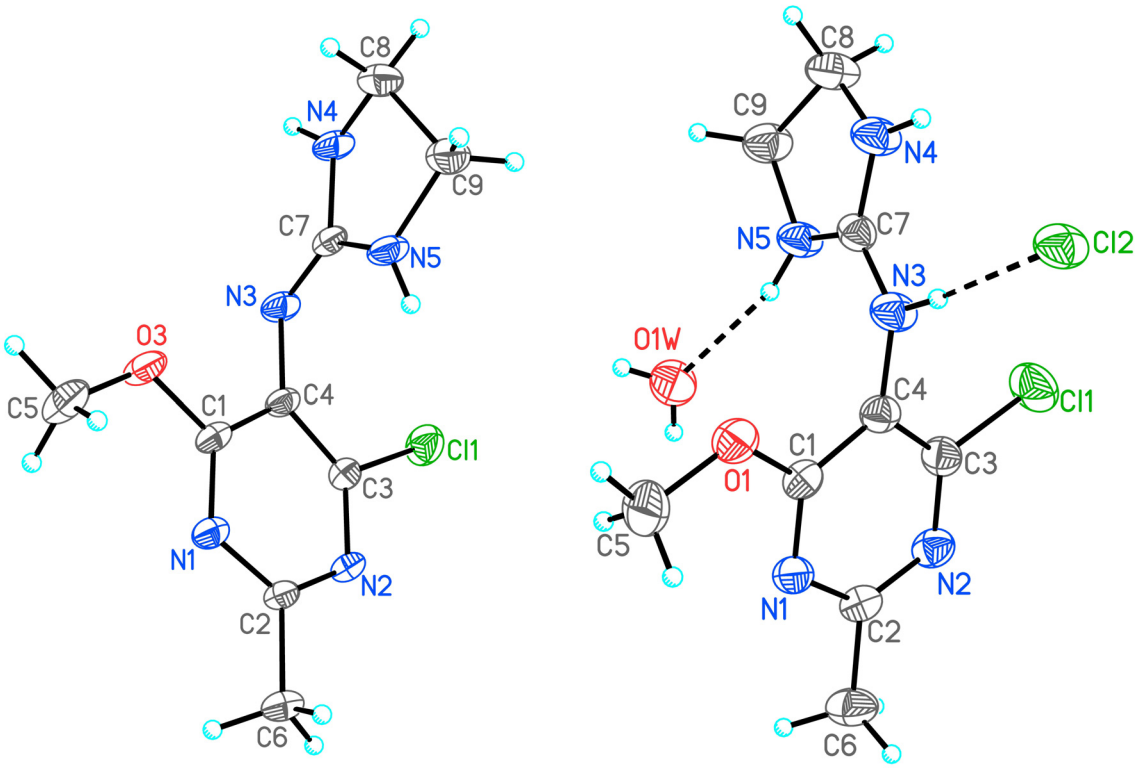

(a) (b)

Figure 2. ORTEP diagrams with the atom labeling. The thermal ellipsoids are drawn at 30% probability. Hydrogen atoms are shown as spheres of arbitrary radii. (a) Moxonidine. (b) Moxonidine hydrochloride monohydrate. Dotted lines represent hydrogen bonding interactions with the chloride and water.

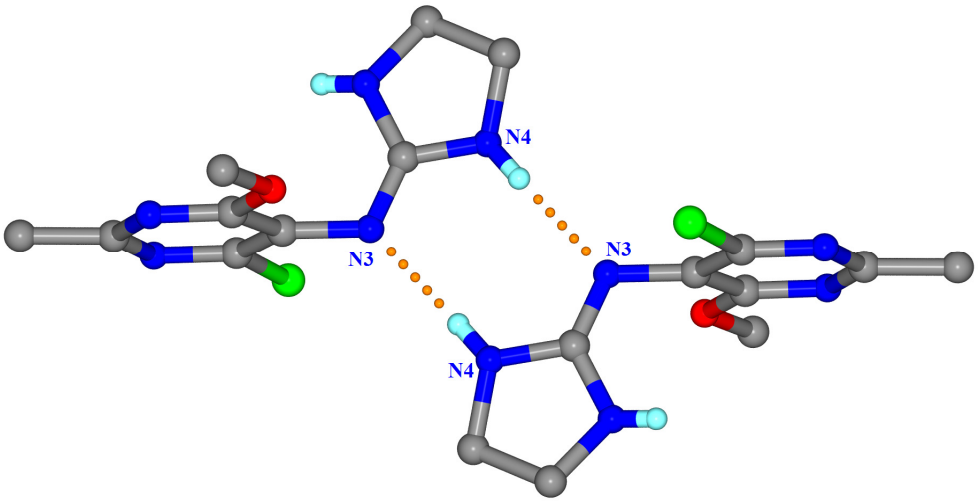

(a)

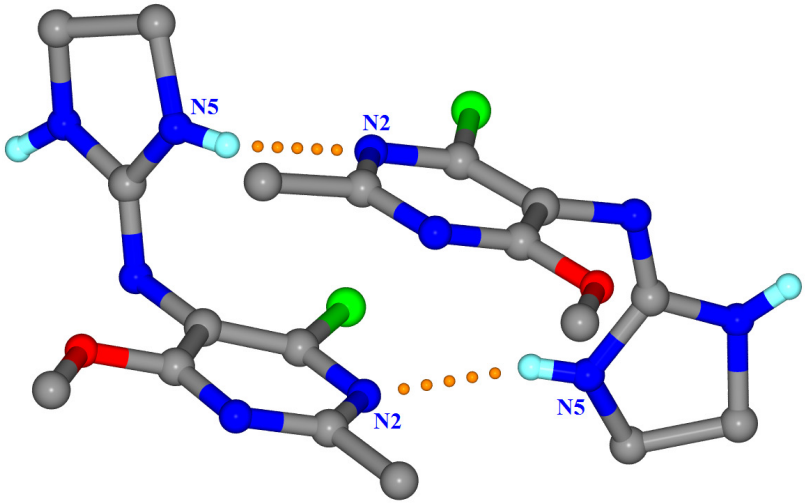

(b)

Figure 3. (a) Imidazolidine…imidazolidine homo dimer in (I), sustained by N-H…N interactions. (b) Imidazolidine…pyrimidine hetero dimer in (I), sustained by N-H…N interactions. Please see table 3 for symmetry codes.

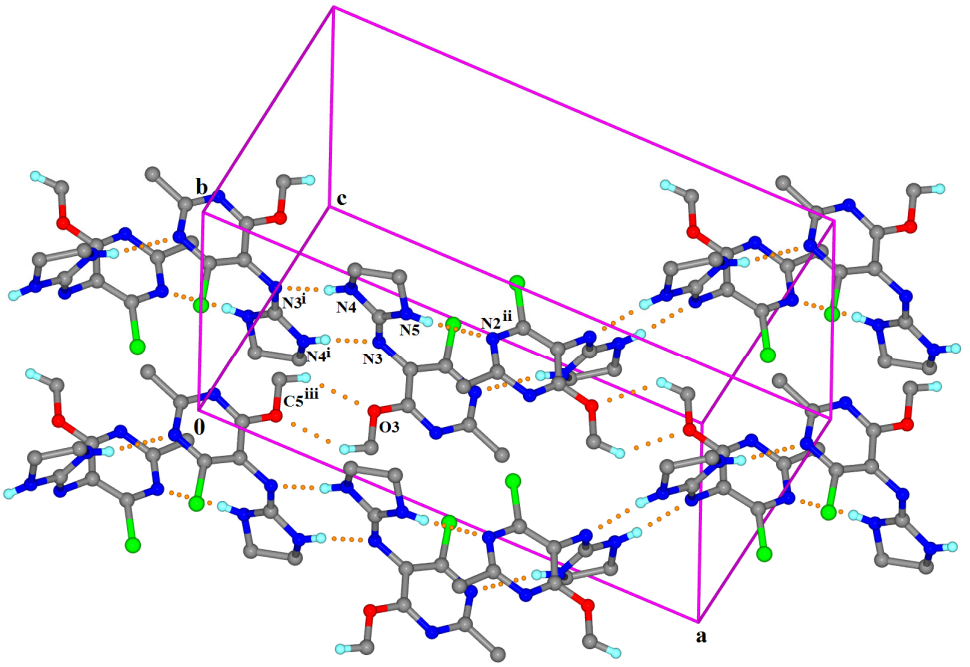

(a)

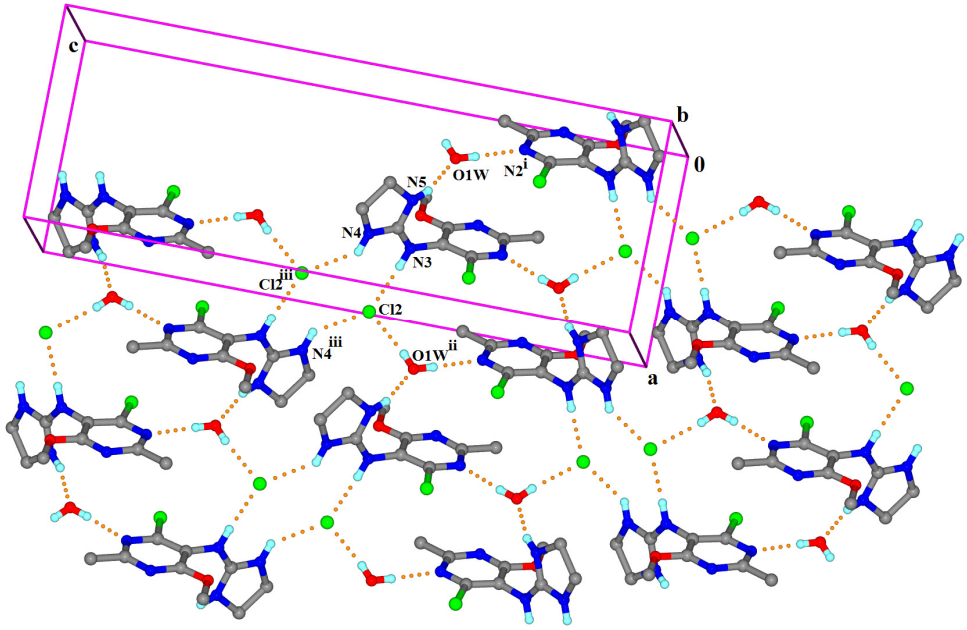

(b)

Figure 4. Part of the unit cell depicting the two dimensional assembly in (a) moxonidine and (b) moxonidine hydrochloride monohydrate. Please see table 3 for symmetry codes.

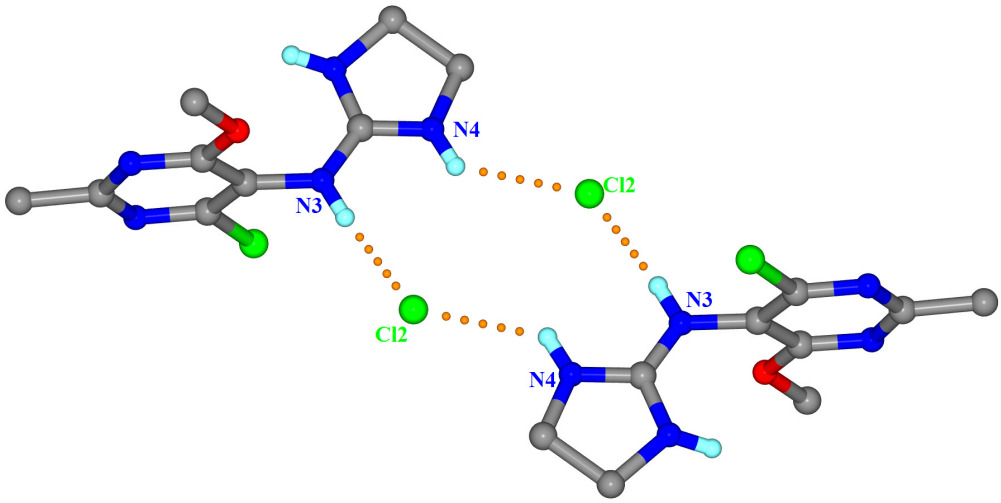

(a)

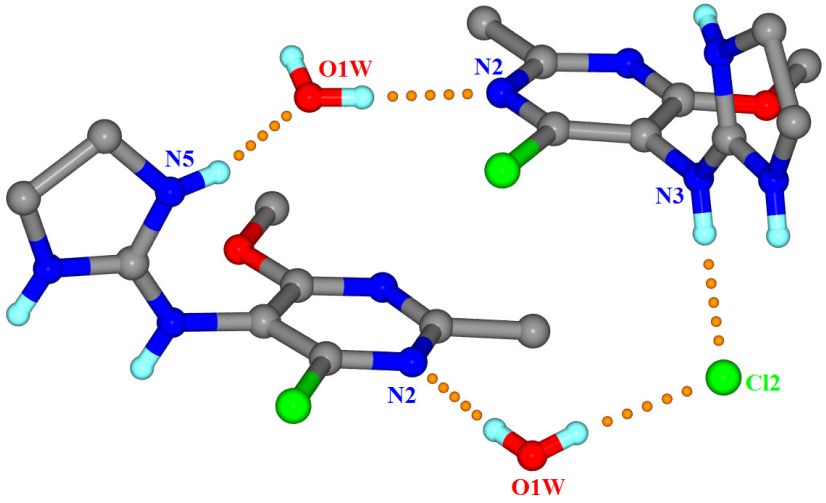

(b)

Figure 5. (a) Chloride ion bridged imidazolidinium homo dimer in (II), sustained by four N-H…Cl interactions. (b) Water and chloride ion bridged imidazolidinium…pyrimidine hetero dimer in (II), sustained by combination of N-H…O, O-H…N, N-H…Cl, and O-H…Cl interactions. Please see table 3 for symmetry codes.

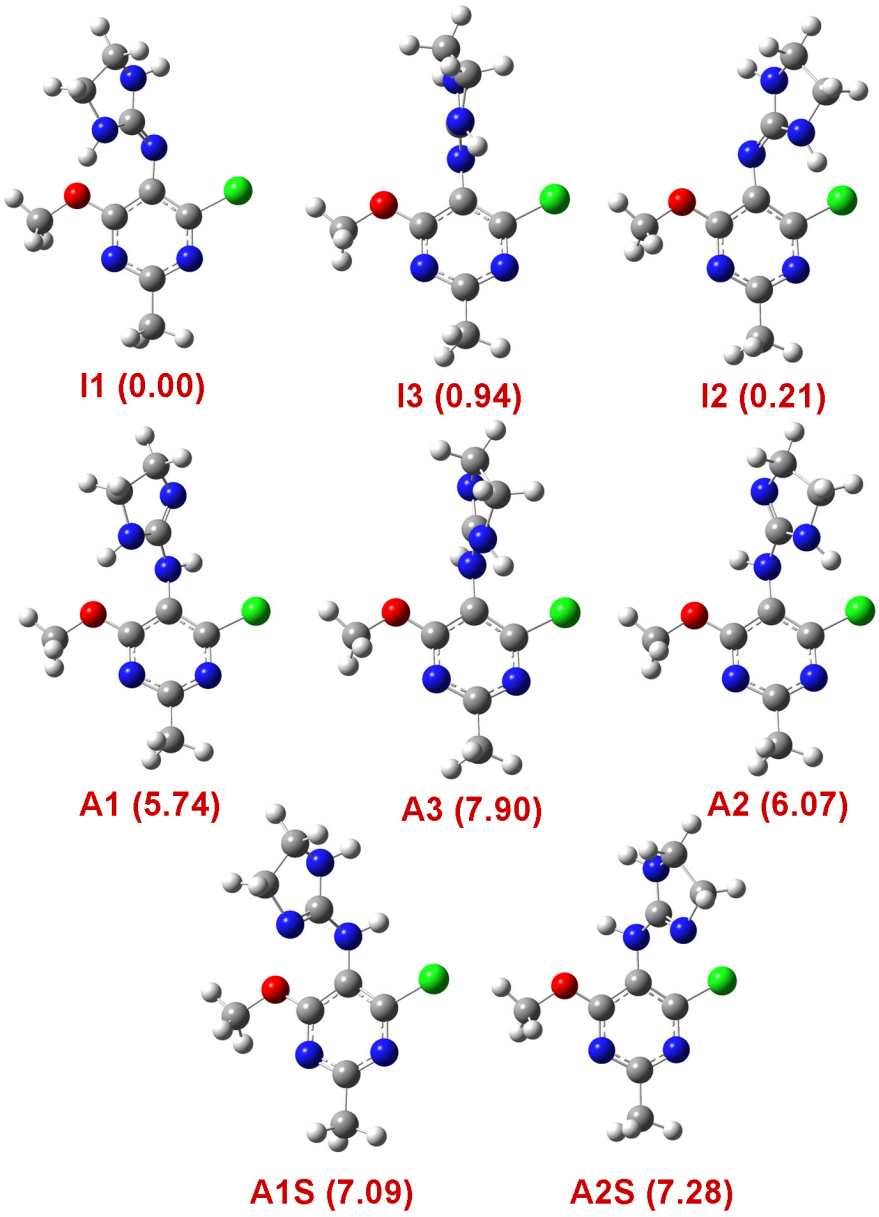

Figure 6. Tautomers/conformations of moxonidine - I1, I2, and I3 are imino and A1, A2, A3 are amino tautomers. The endocyclic and exocyclic N-H of cyclic guanidine are *anti* oriented, however, they can also be *syn* oriented as in A1S and A3S respectively. Relative energies of these tautomer/conformations are provided in the parenthesis.

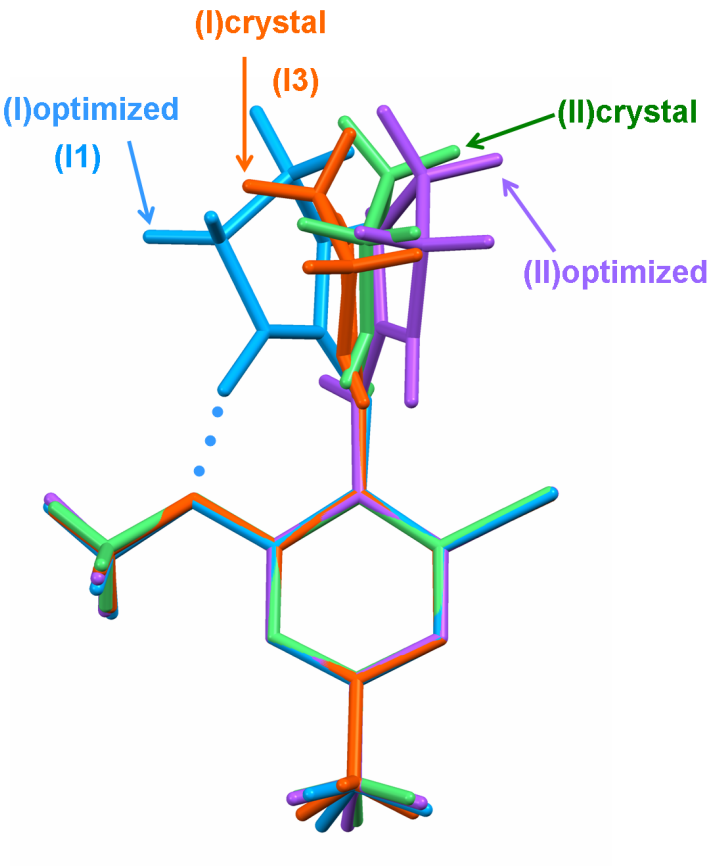

Figure 7. An overlay diagram of crystal and optimized conformations of moxonidine. Conformations are labeled as (I)crystal (orange), (II)crystal (green) for solid state observed conformations in moxonidine and moxonidine HCl salt, respectively and their gas phase optimized conformations are (I)optimized (blue) and (II)optimized (purple). Overlay is made with the pyrimidine ring. The RMS deviation is 0.0116 for (I)crystal & (I)optimized, 0.0166 for (I)crystal & (II)crystal and 0.0198 for (I)crystal & (II)optimized. N-H…O hydrogen bond between imidazolidine NH and methoxy O atom is indicated by dotted lines (H…O distance, 2.16Å, N…O distance, 2.888Å; N-H…O bond angle, 127.3˚) in (I)optimized conformation.

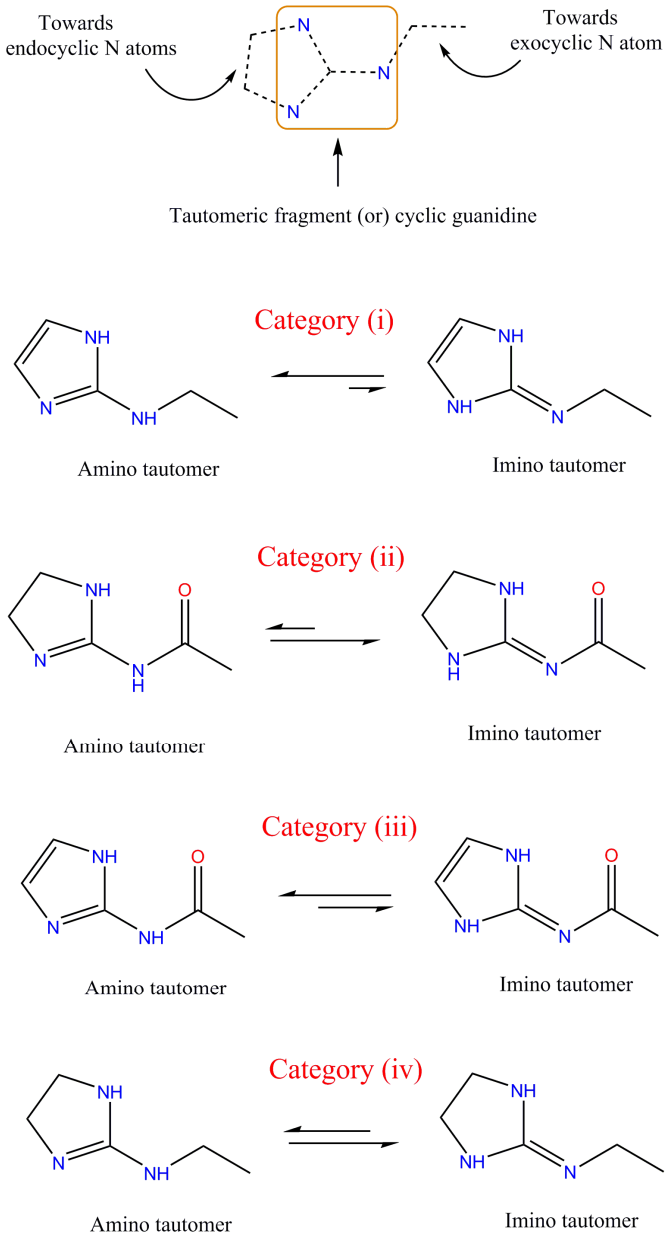

Figure 8. Segregation of 180 structures into four categories depending on the location of additional double bond, i.e. towards exocyclic or endocyclic. Category (i) structures contain the double bond exclusively towards endocyclic N atoms, category (ii) structures contain the double bond exclusively towards exocyclic N atom, category (iii) structures contain the double bonds towards endo as well as exocyclic N atoms and category (iv) structures are without double bonds towards both endo and exo sides. Equilibrium arrows are shown in accordance with tautomeric probabilities obtained from CSD analysis.

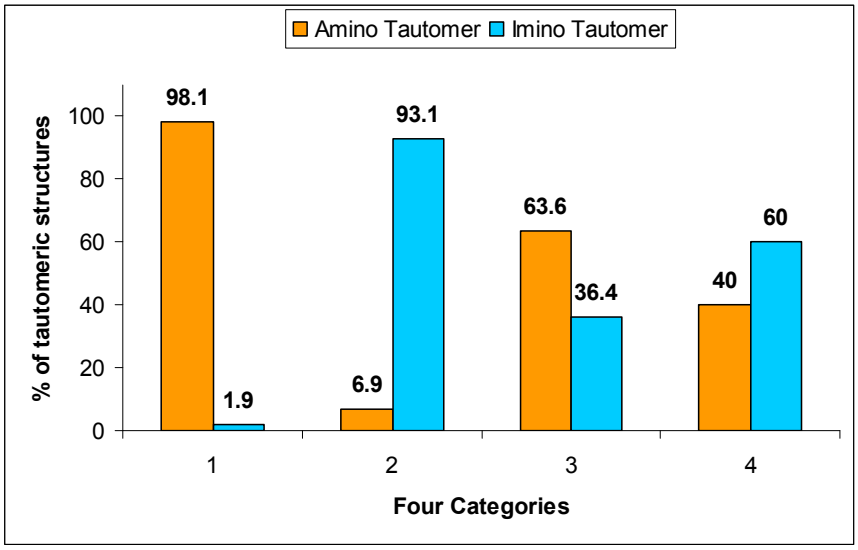

Figure 9. Estimated tautomer probability in four categories of structures. Only one type of tautomer is predominantly observed in categories (i) and (ii) whereas the tautomeric competition is greater in categories (iii) and (iv).

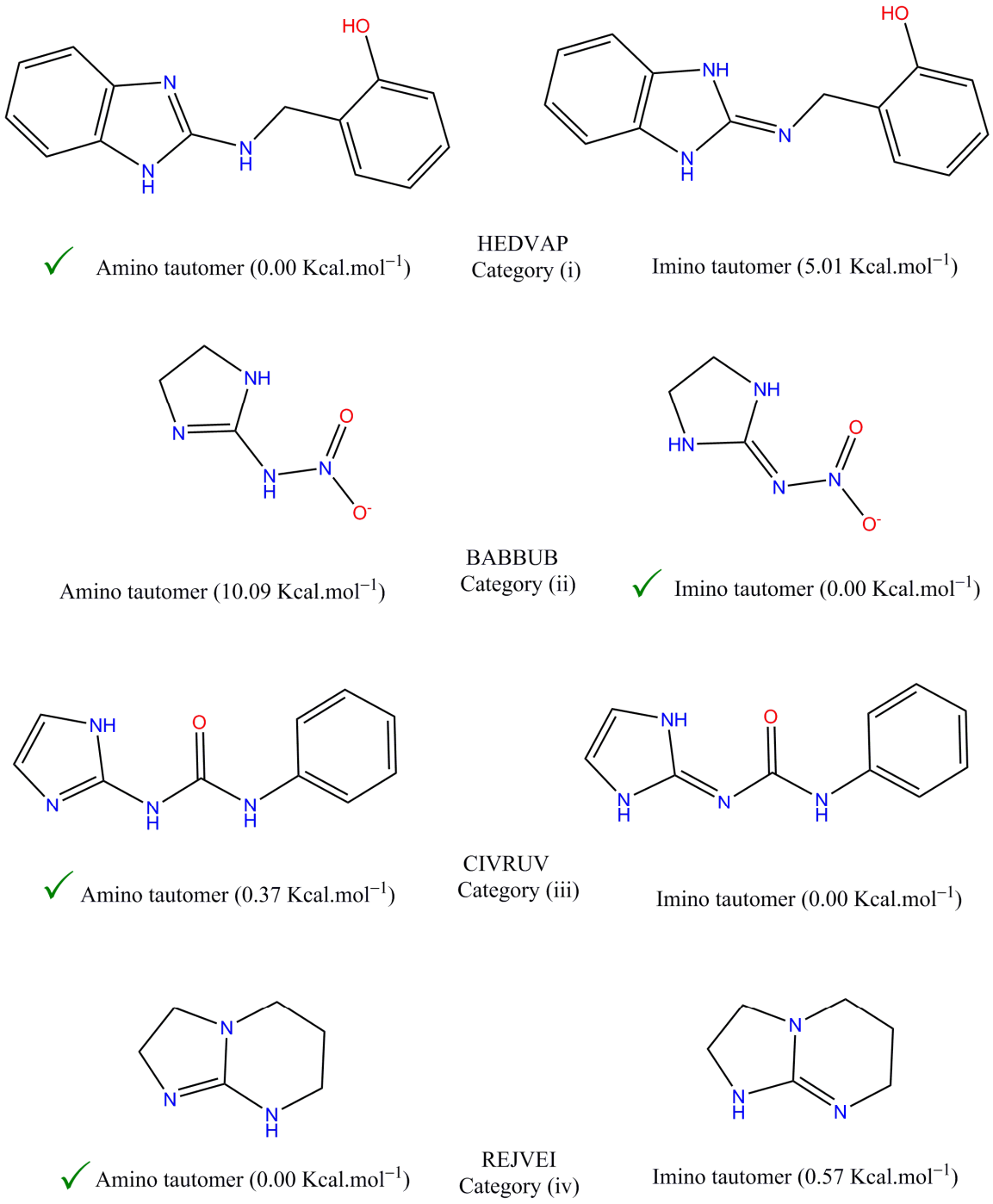

Figure 10. Relative tautomer energies are shown for representative examples from four categories of structures. Tick mark points to the observed tautomer in the crystal structure.

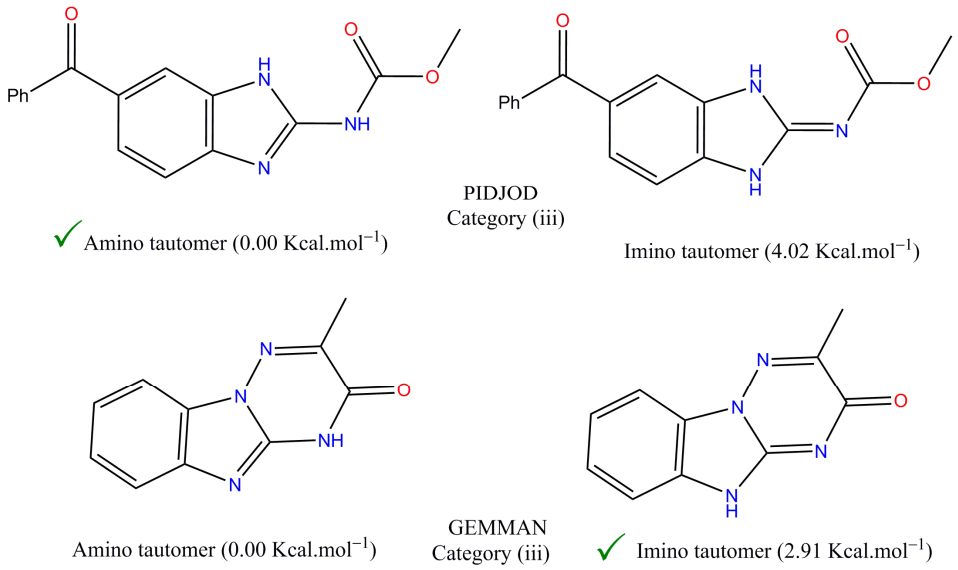

Figure 11. Relative tautomer energies are shown for two selected examples from category (iii) structures. Tick mark points to the observed tautomer in the crystal structure. The more stable amino tautomer is seen in the crystal of PIDJOD whereas the less stable imino tautomer is stabilized in GEMMAN.

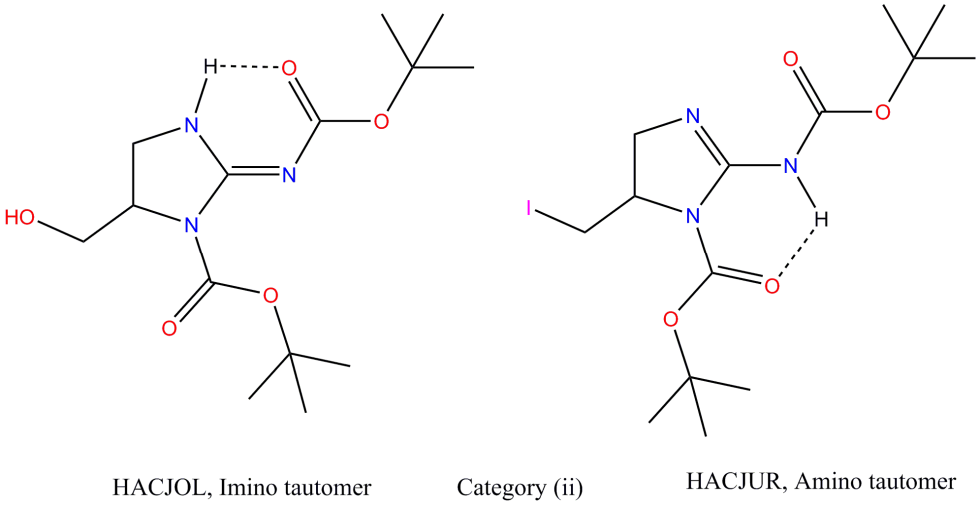

Figure 12. Molecular diagrams of HACJOL and HACJUR which differ in the hydroxyl ↔ iodine substitution. The observed tautomer in the crystal is imino in HACJOL and amino in HACJUR. Stabilization from intramolecular N-H…O hydrogen bonds can be seen in both tautomers.

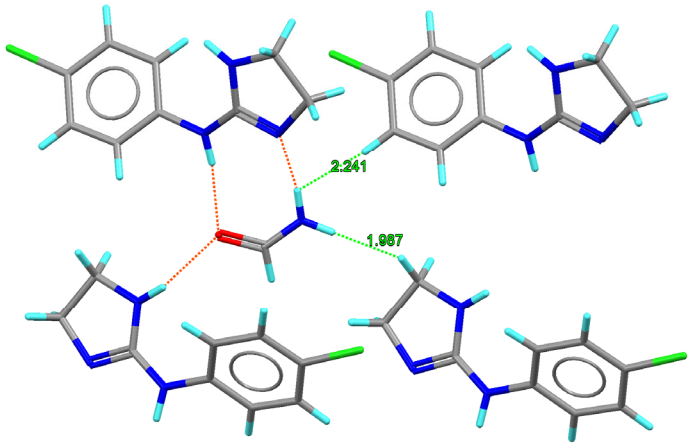

(a)

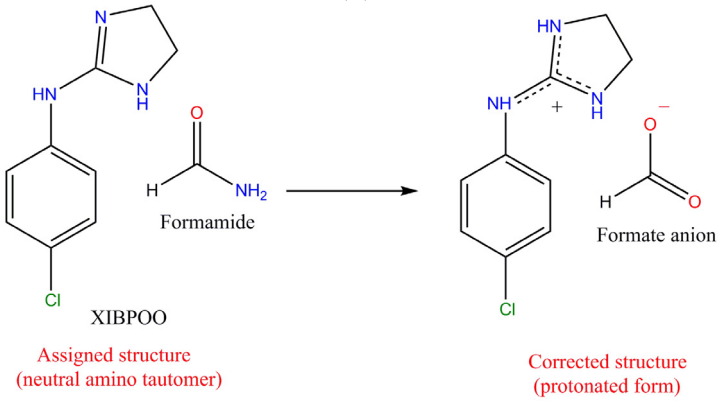

(b)

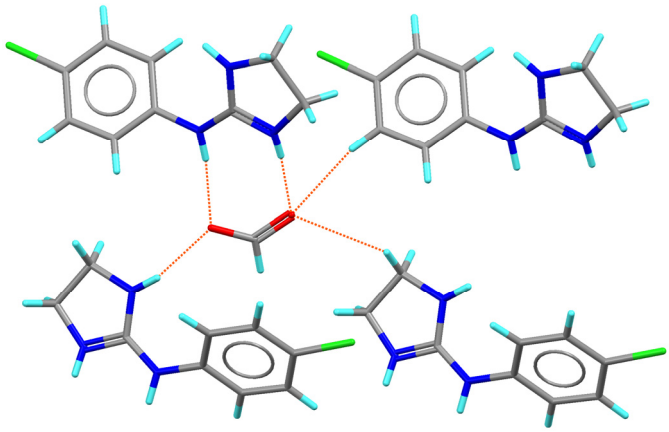

(c)

Figure 13. (a) Molecular packing in the reported crystal structure of XIBPOO. (b) Schematic representation of structure correction in XIBPOO. (c) Molecular packing in the revised crystal structure of XIBPOO. Repulsive H…H contacts of formamide NH are replaced as stabilizing C-H…O contacts of formate anion.

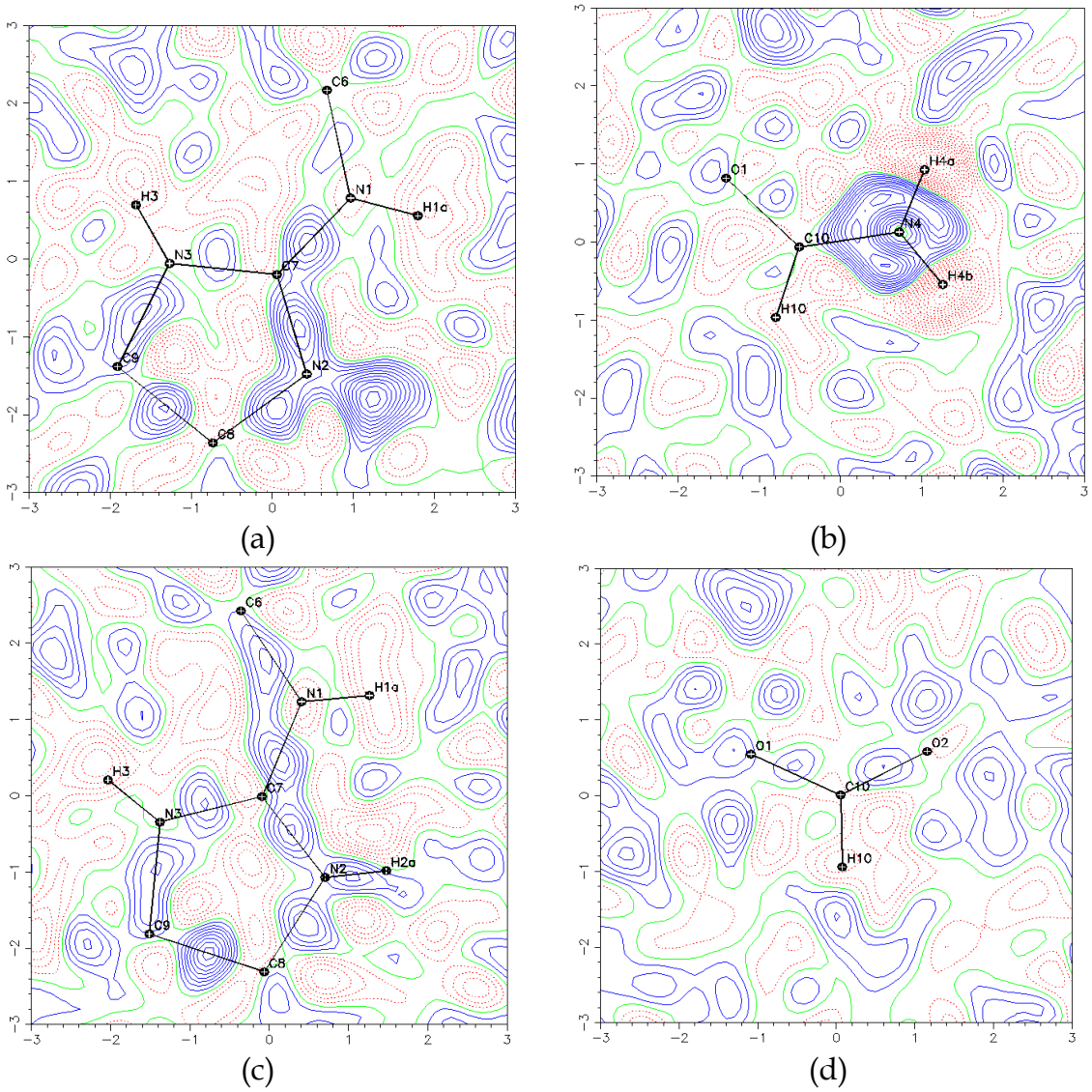

Figure 14. Difference Fourier maps (F_o-F_c) sliced in the plane of (a) imidazoline ring in the reported XIBPOO, (b) formamide in the reported XIBPOO, (c) imidazolidine ring in the revised XIBPOO, (d) formate anion in the revised XIBPOO. Positive contour lines are shown in solid blue lines, negative contour lines in dotted red lines, and zero contour lines are indicated in solid green lines. The contour intervals are drawn at 0.05 eÅ^{-3}.

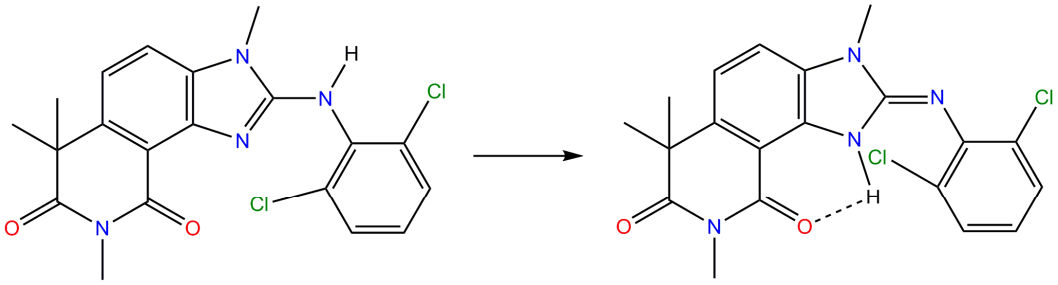

(a)

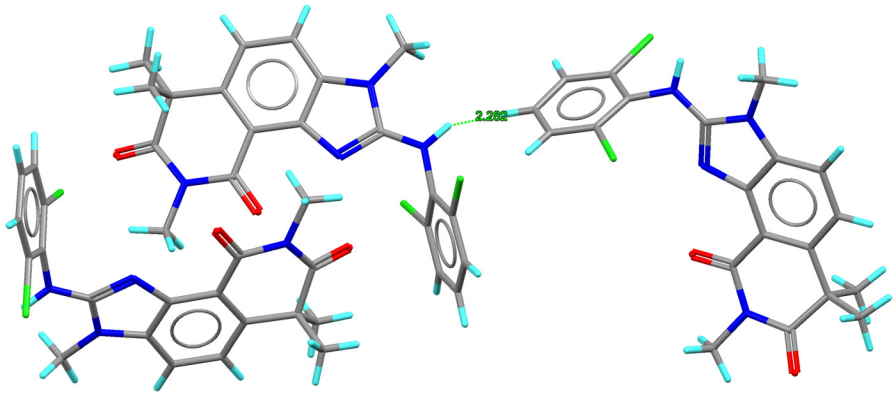

(b)

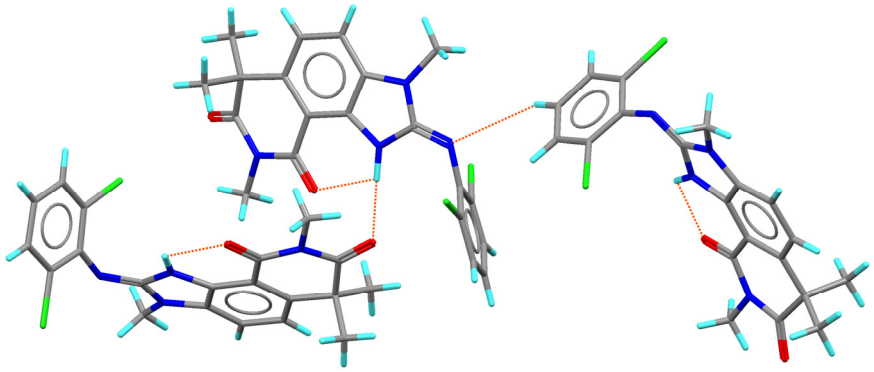

(c)

Figure 15. (a) Schematic representation of QABDON tautomer correction from amino to imino. (b) Molecular packing in the reported crystal structure of QABDON. (b) Molecular packing in the revised crystal structure of QABDON. Repulsive H…H contacts are replaced by stabilizing N-H…O and C-H…N interactions in the revised structure.